

# RACCoON: A VERSATILE INSTRUCTIONAL VIDEO EDITING FRAMEWORK WITH AUTO-GENERATED NARRATIVES

**Anonymous authors**

Paper under double-blind review

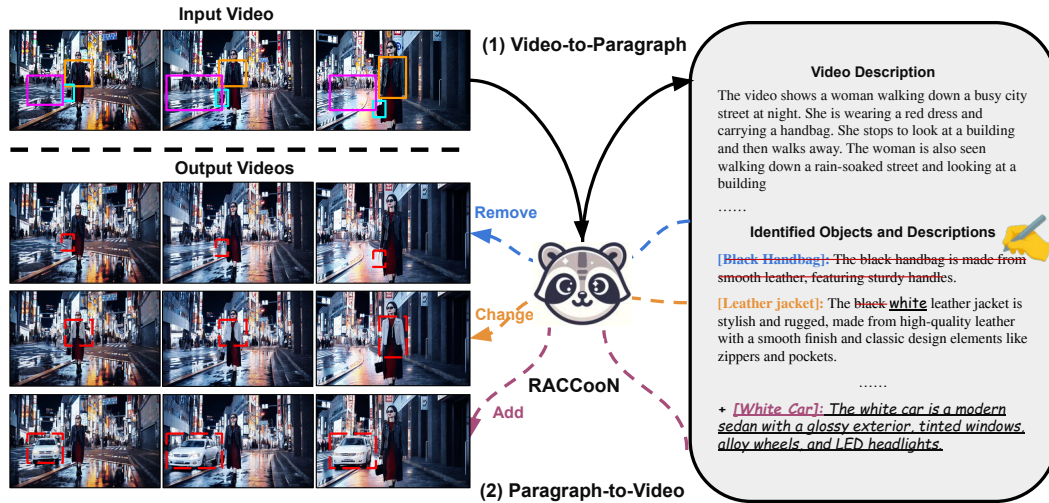


Figure 1: **Overview of RACCoON**, a versatile and user-friendly video-to-paragraph-to-video framework, enables users to remove, add, or change video content via updating auto-generated narratives.

## ABSTRACT

Recent video generative models primarily rely on carefully written text prompts for specific tasks, like inpainting or style editing. They require labor-intensive textual descriptions for input videos, hindering their flexibility to adapt personal/raw videos to user specifications. This paper proposes **RACCoON**, a versatile and user-friendly **video-to-paragraph-to-video** generative framework that supports multiple video editing capabilities such as removal, addition, and modification, through a unified pipeline. RACCoON consists of two principal stages: *Video-to-Paragraph* (V2P) and *Paragraph-to-Video* (P2V). In the V2P stage, we automatically describe video scenes in well-structured natural language, capturing both the holistic context and focused object details. Subsequently, in the P2V stage, users can optionally refine these descriptions to guide the video diffusion model, enabling various modifications to the input video, such as removing, changing subjects, and/or adding new objects. The proposed approach stands out from other methods through several significant contributions: (1) RACCoON suggests a multi-granular spatiotemporal pooling strategy to generate well-structured video descriptions, capturing both the broad context and object details without requiring complex human annotations, simplifying precise video content editing based on text for users. (2) Our video generative model incorporates auto-generated narratives or instructions to enhance the quality and accuracy of the generated content. (3) RACCoON also plans to imagine new objects in a given video, so users simply prompt the model to receive a detailed video editing plan for complex video editing. The proposed framework demonstrates impressive versatile capabilities in video-to-paragraph generation (up to 9.4%  $\uparrow$  absolute improvement in human evaluations against the baseline), video content editing (relative 49.7%  $\downarrow$  in FVD), and can be incorporated into other SoTA video generative models for further enhancement.

054 **1 INTRODUCTION**

055

056 Recent advances in video generative models (Yan et al., 2021; Hong et al., 2022; Esser et al., 2023;  
 057 Mei & Patel, 2023; Chai et al., 2023; Ceylan et al., 2023; Blattmann et al., 2023; Wu et al., 2023a),  
 058 including Sora (openai, 2024), have demonstrated remarkable capabilities in creating high-quality  
 059 videos. Simultaneously, video editing models (Geyer et al., 2023; Qi et al., 2023; Wang et al., 2024b;  
 060 Yu et al., 2023; Wu et al., 2024; Zhang et al., 2023b) have gained significant attention, thanks to their  
 061 promising applications that allow users to modify videos according to *user-written* textual instructions,  
 062 effectively altering video content and attributes. Despite these advancements, significant challenges  
 063 remain in developing a versatile and user-friendly framework that facilitates easy video modification  
 064 for personal use. The primary challenges include: 1) the complexity of training a unified framework  
 065 encompassing multiple video editing skills (e.g., remove, add, or change an object). Training a single  
 066 model to perform various editing skills is highly challenging, and recent video editing methods often  
 067 focus on specific tasks, such as background inpainting (Yu et al., 2023; Wu et al., 2024), or attribute  
 068 editing (Geyer et al., 2023; Qi et al., 2023; Jeong & Ye, 2023). 2) the necessity for well-structured  
 069 textual prompts that accurately describe videos and can be edited to support diverse video editing  
 070 skills. The quality of prompts critically influences the models’ capabilities and the quality of their  
 071 outputs. Generating detailed prompts is time-consuming and costly, and the quality varies depending  
 072 on the expertise of the annotators. Although Multimodal Large Language Models (MLLMs) (Liu  
 073 et al., 2023b; Munasinghe et al., 2023; Yang et al., 2023; Yu et al., 2024) have been explored for  
 074 automatically describing videos, they often overlook critical details in complex scenes. This oversight  
 075 compromises the development of a seamless pipeline, hindering both user convenience and the  
 effectiveness of video generative models.

076 To tackle these limitations, as shown in Fig. 1, we introduce **RACCooN: A Versatile Instructional**  
 077 **Video Editing Framework with Auto-Generated Narratives**, a novel **video-to-paragraph-to-video**  
 078 (**V2P2V**) generative framework that facilitates diverse video editing (Remove, Add, and Change)  
 079 capabilities based on auto-generated narratives. RACCooN allows for the seamless removal and  
 080 modification of subject attributes, as well as the addition of new objects to videos **without requiring**  
 081 **densely annotated video prompts or extensive user planning**. Our framework operates in  
 082 two main stages: *video-to-paragraph* (V2P) and *paragraph-to-video* (P2V). In the V2P stage, we  
 083 introduce a new video descriptive framework built on a pre-trained Video-LLM backbone (PG-  
 084 Video-LLaVA (Munasinghe et al., 2023)). We find that existing Video-LLMs effectively capture  
 085 holistic video features, yet often overlook detailed cues that are critical for accurate video editing,  
 086 as users may be interested in altering these missing contexts. To address this, we propose a novel  
 087 multi-granular video perception strategy that leverages superpixels (Li & Chen, 2015; Ke et al., 2023)  
 088 to capture diverse and informative localized contexts throughout a video. We first extract fine-grained  
 089 superpixels using a lightweight predictor (Yang et al., 2020) and then apply overlapping k-means  
 090 clustering (Cleuziou, 2007; Whang et al., 2015; Khanmohammadi et al., 2017) to segment visual  
 091 scenes into various levels of granularity. The suggested localized spatiotemporal segmentation assists  
 092 the LLM’s comprehension of objects, actions, and events within the video, enabling it to generate  
 093 fluent and detailed natural language descriptions. Next, in the P2V stage, to integrate multiple editing  
 094 capabilities into a single model, we fine-tuned a video inpainting model that can paint video objects  
 095 accurately with detailed text, object masks, and condition video. Then, by utilizing user-modified  
 096 prompts from generated descriptions in the V2P stage, our video diffusion model can accurately *paint*  
 097 corresponding video regions, ensuring that textual updates from prompts are reflected in various  
 098 editing tasks. Moreover, to better support our model training, we have collected the **Video Paragraph**  
 099 with **Localized Mask** (**VPLM**) dataset—a collection of over 7.2K high-quality video-paragraph  
 099 descriptions and 5.5k detailed object descriptions with masks, annotated from the publicly available  
 dataset using GPT-4V (Achiam et al., 2023).

100 We emphasize that RACCooN enhances the quality and versatility of video editing by leveraging  
 101 detailed, automatically generated textual prompts that minimize ambiguity and refine the scope of  
 102 generation. We validate the extensive capabilities of the RACCooN framework in both V2P genera-  
 103 tion, text-based video content editing, and video generation on ActivityNet (Krishna et al., 2017),  
 104 YouCook2 (Zhou et al., 2018a), UCF101 (Soomro et al., 2012), DAVIS (Pont-Tuset et al., 2017), and  
 105 our proposed VPLM datasets. On the V2P side, RACCooN outperforms several strong video cap-  
 106 tioning baselines (Li et al., 2023; Munasinghe et al., 2023; Liu et al., 2023b), particularly improving  
 107 by average **+9.1%<sup>p</sup>** on VPLM and up to **+9.4%<sup>p</sup>** on YouCook2 compared to PG-VL (Munasinghe  
 et al., 2023), based on both automatic metrics and human evaluation. On the P2V side, RACCooN

surpasses previous strong video editing/inpainting baselines (Geyer et al., 2023; Qi et al., 2023; Wang et al., 2024b; Yu et al., 2023; Wu et al., 2024) over three subtasks of video content editing (remove, add, and change video objects) over 9 metrics. We also demonstrate that the proposed RACCoN framework can enhance SoTA video generative models by leveraging detailed auto-generated textual prompts. We further conduct extensive ablation and visualizations to validate the improvement quantitatively and qualitatively. Our contributions are as follows:

1. **Framework Contribution:** RACCoN offers a user-friendly and unified framework for various video editing tasks. It provides improved interpretability and interactive experiences by automatically generating detailed, object-centric video descriptions and layout plans tailored to different editing objectives, which cannot be done through a simple combination of existing models.
2. **Technical Contribution:** We present a novel **multi-granular pooling** strategy to capture local video contexts, enhancing video comprehension by generating fluent and detailed descriptions in a zero-shot setting. This enables users to create new videos that retain the visual characteristics of the input and focus on specific context editing.
3. **Training/Dataset Contribution:** To enable RACCoN to follow complex and varied user requests for video editing, we present the **VPLM** dataset, which contains 7.2K high-quality detailed video paragraphs and 5.5K object-level detailed caption-mask pairs. This dataset facilitates accurate V2P and P2V stages with high-quality, localized textural prompts and videos.

## 2 RELATED WORK

**Video-to-Paragraph Generation.** The recent trend in video-language tasks focuses on generating comprehensive textual descriptions for long and complex video content (Shen et al., 2017; Krishna et al., 2017; Wang et al., 2018; Tewel et al., 2022; Wu et al., 2023b). Vid2Seq (Yang et al., 2023) introduces a novel dense event captioning approach for narrated videos, with time tokens and event boundaries. Video-LLaVA variants (Lin et al., 2023a; Munasinghe et al., 2023) present a large multimodal model integrating text, video, and audio inputs for generative and question-answering tasks. Similarly, LLaVA-Next (Zhang et al., 2024) improves zero-shot video understanding by transferring multi-image knowledge through concatenated visual tokens. While these methods are effective in video description, they often miss key contextual details (Zhang et al., 2023a; Li et al., 2023). Our RACCoN captures both holistic and localized details by leveraging localized spatiotemporal information, enhancing video editing and generation capabilities.

**Prompt-to-Video Editing.** Video editing (Ceylan et al., 2023; Liu et al., 2023c; Couairon et al., 2023; Kondratyuk et al., 2023; Wang et al., 2023; Zhang et al., 2023c) involves enhancing, modifying, or manipulating video content for desired effects. VideoComposer (Wang et al., 2024b) offers a multi-source controllable video generative framework. TokenFlow (Geyer et al., 2023) adapts text-to-image diffusion with flow matching for consistent text-driven video editing. LGVI (Wu et al., 2024) integrates an MLLM for complex language-based video inpainting. These methods often focus on specific tasks and may inadvertently alter unrelated regions due to limited contextual information. Our V2P2V framework overcomes these limitations by using auto-generated, detailed descriptions to integrate key contexts into diverse editing tasks.

## 3 RACCOON: A VERSATILE INSTRUCTIONAL VIDEO EDITING FRAMEWORK WITH AUTO-GENERATED NARRATIVES

Conditional video generation and editing models struggle with complex scenes due to vague text descriptions and limited video understanding. Despite improvements from recent advances in MLLMs, these models still struggle to capture complex spatial-temporal dynamics, often omitting crucial objects and details. Training a text-to-video model with such vague prompts compromises output specificity, and leads the model to generate average, arbitrary content that fails to capture user instructions’ nuances. To address these issues, we introduce RACCoN, a user-friendly, two-stage video-to-paragraph-to-video editing framework. Initially, RACCoN generates detailed, structured paragraphs from videos, capturing holistic content and key local objects through multi-granular spatiotemporal information. These detailed descriptions are then used for conditional video generation and editing, enabling users to add, remove, or change video objects directly by interacting with the generated descriptions, thus enhancing the specificity and relevance of the output.

162

163

164

165

166

167

168

169

170

171

172

173

174

175

176

177

**Figure 2: Illustration of RACCoN framework.** RACCoN generates video descriptions with the three distinct pooled visual tokens, including Multi-Granular Spatiotemporal (MGS) Pooling. Next, users can edit the generated descriptions by adding, removing, or modifying words to create new videos. Note that for adding object tasks, if users do not provide layout information for the objects they want to add, RACCoN can predict the target layout in each frame.

178

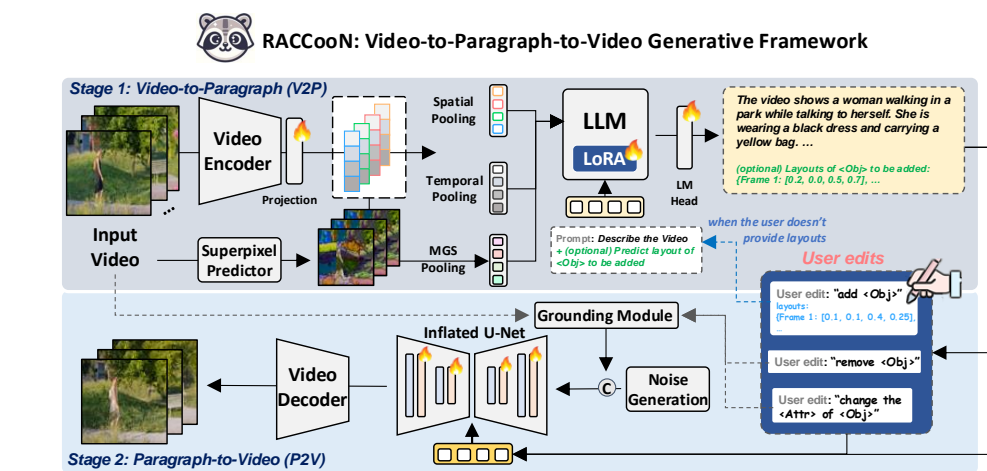
179

180

181

182

183



### 3.1 V2P: AUTO-DESCRIPTIVE FRAMEWORK WITH MULTI-GRANULAR VIDEO PERCEPTION

184

185

186

187

188

189

190

191

192

193

194

195

196

197

198

199

200

201

202

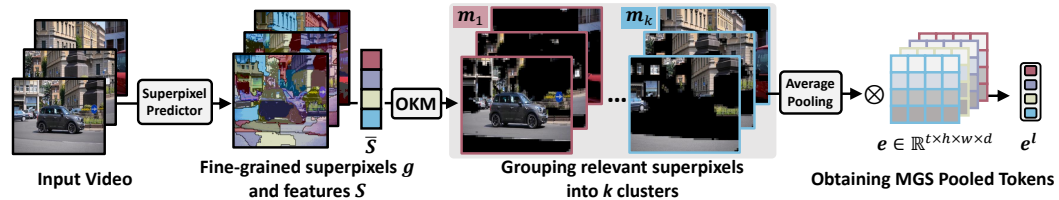
203

204

205

206

**Multimodal LLM for Video Paragraph Generation.** In the V2P stage, the RACCoN framework generates well-structured, detailed descriptions for both holistic videos and local objects. It employs a multimodal LLM with three main components: a visual encoder  $E$ , a multimodal projector, and an LLM. Given an input video  $\mathbf{x} \in \mathbb{R}^{F \times C \times H \times W}$ , where  $F$ ,  $C$ ,  $H$ , and  $W$  represent the number of frames, channels, height, and width, respectively, we extract video features using the visual encoder:  $\mathbf{e} = E(\mathbf{x}) \in \mathbb{R}^{t \times h \times w \times d}$ . Here,  $t$ ,  $h$ ,  $w$ , and  $d$  denote the encoded temporal dimension, the height and width of the tokens, and the feature dimension. To understand complex videos with multiple scenes, we use three pooling strategies: *spatial pooling*, *temporal pooling*, and *multi-granular spatiotemporal pooling*. Spatial pooling  $\mathbf{e}^s = \text{Pooling}^s(\mathbf{e}) \in \mathbb{R}^{t \times d}$  aggregates tokens within the same frame, while temporal pooling  $\mathbf{e}^t = \text{Pooling}^t(\mathbf{e}) \in \mathbb{R}^{(h \cdot w) \times d}$  averages features across the temporal dimension for the same region. Despite these strategies helping the LLM grasp the video holistically in space or time, they often overlook capturing key objects or actions localized throughout the video stream, especially in untrimmed, dynamic, multi-scene videos.



207

208

209

210

211

212

213

214

215

**Figure 3: Illustration of MGS pooling.** We obtain MGS pooling tokens using a spatiotemporal mask  $\mathbf{m}$  via overlapping k-means clustering (OKM) of averaged superpixel features  $\bar{\mathbf{S}}$ .

**Multi-Granular Spatiotemporal Pooling.** To address this issue, we introduce a novel superpixel-based spatiotemporal pooling strategy, coined *multi-granular spatiotemporal pooling* (MGS pooling). As illustrated in Fig. 2 left top, this strategy is designed to capture localized information via superpixels across spatial and temporal dimensions. Superpixels (Li & Chen, 2015; Giordano et al., 2015; Yang et al., 2020; Ke et al., 2023) are small and coherent clusters of pixels that share similar characteristics, such as color or texture. These clusters provide an efficient representation of visual scenes and are resilient to frame noise since they average out the pixel values within each cluster, effectively smoothing out variations induced by noise. As shown in Fig. 3, we use a lightweight superpixel predictor  $\sigma(\cdot)$  (Yang et al., 2020) to generate superpixels across video frames, capturing the granular visuality of each local area. However, due to their limited coverage area, these fine-grained visual

216 features often fail to capture attribute-level semantics, such as objects and actions (Zhang et al.,  
 217 2023a; Li et al., 2023). Motivated by the importance of varying the compositions of multiple  
 218 superpixels for different contexts in video understanding, we propose the use of overlapping k-means  
 219 clustering (Cleuziou, 2007; Whang et al., 2015) for the obtained video superpixels, which improves  
 220 the granularity from fine to coarse. This approach allows the LLM to gather informative cues about  
 221 various objects and actions. We first obtain the pixel features and the superpixel index vector for  
 222 the video pixels:  $S, g = \sigma(x, g_{\text{init}})$ , where  $g_{\text{init}}$  is the input superpixel indices, initialized by a  
 223 region-based grid. Given the averaged pixel features of each superpixel,  $\bar{S} \in \mathbb{R}^{|g| \times d_s}$ , where  $d_s$   
 224 denotes the pixel feature size, we generate the MGS tokens  $e^l$ :

$$\begin{aligned} m &= \text{OKM}(\bar{S}, k, v) \in \{0, 1\}^{k \times F \times H \times W}, \\ e^l &= \text{AvgPool}(m) \otimes e \in \mathbb{R}^{k \times d}, \end{aligned} \quad (1)$$

225 where OKM represents the overlapping k-means algorithm with  $k$  centroids and overlap scale  $v$  for  
 226 each cluster.  $m$  denotes the set of binary masks for superpixels.  $\otimes$  denotes tensor multiplication.  
 227 We describe the detailed MGS process and ablation of pooling strategies in the Appendix. Next,  
 228 we concatenate the pooled video tokens and map them into the text embedding space using the  
 229 multimodal linear projector. Combined with the embedding of the encoded text token  $e^p$  from the  
 230 textual prompt, the LLM generates a well-structured and detailed description  $a$  of the video:

$$\hat{e} = \text{CONCAT}[e^s; e^l; e^t] \cdot W^\top, \quad a = LLM(\text{CONCAT}[e^p; \hat{e}]), \quad (2)$$

231 where  $W \in \mathbb{R}^{d \times d'}$  is the weight matrix for linear projection into the text embedding dimension  $d'$ .  
 232 We highlight that our video description framework serves as an integrated, user-interactive tool for  
 233 video-to-paragraph generation and video content editing. (Fig. 2 top right).

### 240 3.2 P2V: USER-INTERACTIVE VIDEO EDITING WITH AUTO-GENERATED DESCRIPTIONS

241 With the well-structured, detailed, and object-centric video description generated from the *Video-to-*  
 242 *Paragraph* stage, users can ‘read’ the video details and interactively modify the content by altering the  
 243 model-generated description. This approach shifts users’ focus from labor-intensive video observation  
 244 to content editing. We categorize general video content editing into three important subtasks: **(1)**  
 245 **Video Object Adding:** add extra objects to a video. **(2) Video Object Removing:** delete target  
 246 objects and re-generate the object region as the background. **(3) Video Object Changing:** change  
 247 objects’ attributes (e.g., color, textural, material). Many previous works have made great progress  
 248 in video editing (Wu et al., 2024; Geyer et al., 2023; Qi et al., 2023; Zhang et al., 2023b; Fan et al.,  
 249 2024) but usually focus on one of these subtasks. In this paper, we propose a unified generative model  
 250 for video content editing that integrates all those crucial subtasks. Specifically, we formulate these  
 251 subtasks as text-based video painting tasks and leverage a single video diffusion model for adding,  
 252 removing, and changing video objects in the form of inpainting.

253 As shown in Fig. 2 bottom, our video diffusion model processes input video  $x \in \mathbb{R}^{F \times C \times H \times W}$  with  
 254 a predicted binary mask  $m' \in \mathbb{R}^{F \times 1 \times H \times W}$  targeting specific regions for modification. Following  
 255 image inpainting techniques (Xie et al., 2023; Rombach et al., 2022), we apply the mask<sup>1</sup> to the video  
 256 to designate the editing region. The masked video is then encoded using a Variational Autoencoder  
 257 (VAE (Kingma & Welling, 2013)) to serve as the generation condition. The model can then be  
 258 informed on which video region should be edited for localized editing. Driven by the detailed  
 259 description, the diffusion model can conduct diverse video editing that reflects the text prompts.

260 In addition, we provide details regarding the process of adding objects in video editing. Indeed,  
 261 adding objects can be considered a unique video editing task, distinct from removing objects or  
 262 changing attributes. Unlike the latter scenarios, where the target objects are already present in the  
 263 initial video, adding objects involves introducing entirely new elements, which necessitates a slightly  
 264 different editing process.

265 As illustrated in Fig. 2, the MLLM in the V2P process provides not only detailed descriptions but  
 266 also frame-wise placement suggestions for new objects in the form of bounding box sequences. The  
 267 object insertion process in RACCoN in inference is conducted through the following steps:

268 269 <sup>1</sup>We use image grounding (Liu et al., 2023d) and video tracking models (Cheng et al., 2023) as the off-the-shelf mask predictor in inference.

- 270 1. *User Edit*: The user provides an instruction to add a specific object.  
 271 2. *MLLM Output*: The finetuned MLLM in V2P generates fine-grained video descriptions along with  
 272 frame-wise bounding box suggestions for new objects. For example, “Layouts of <Obj> to be added:  
 273 {Frame 1: [0.2, 0.0, 0.5, 0.7], Frame 2: [0.2, 0.1, 0.4, 0.65], ...}” specifies the layout  
 274 for each frame, where  $[x_1, y_1, x_2, y_2]$  represents the top-left and bottom-right corners of the  
 275 bounding box, with coordinates normalized to the range  $[0, 1]$  (the yellow box in Fig. 2, top right).  
 276 3. *Video editing*: Generate videos based on the MLLM-generated output, including the frame-wise  
 277 layout of the object to be added.

278

### 279 3.3 VPLM DATASET COLLECTION AND RACCoN PIPELINE TRAINING

280

281 **Dataset Collection.** We utilize video datasets (Majumdar et al., 2020; Gavrilyuk et al., 2018)  
 282 from previous video inpainting work (Wu et al., 2024). Each raw video is accompanied by multiple  
 283 inpainted versions with specific objects removed and includes binary masks of these objects. Although  
 284 well-annotated with object masks and inpainted backgrounds, these datasets lack detailed descriptions  
 285 of holistic video and specific local objects, hindering RACCoN’s training for producing well-  
 286 structured captions for video editing. To address this, we use GPT-4V (Achiam et al., 2023) to  
 287 annotate detailed video descriptions. We first re-arrange uniformly sampled video frames into a  
 288 grid-image (Fan et al., 2021) and add visual prompts by numbering each frame. We then ask GPT-4V  
 289 to generate detailed captions for both the entire video and key objects, in a well-structured format.  
 290 Next, we train V2P and P2V stages in our framework separately (Fig. 2). In the end, RACCoN  
 291 can automatically generate detailed, well-structured descriptions for raw videos and adapt these  
 292 descriptions based on user updates for various video content editing tasks.

293 **MLLM Instructional Fine-tuning.** To enable the MLLM to output detailed video descriptions  
 294 for content editing, we construct an instructional fine-tuning dataset based on VPLM with two  
 295 video-instruction (Liu et al., 2023b) designs: (1) For object editing and removal, the MLLM generates  
 296 structured video captions identifying key objects in the original video  $\mathbf{x}$ , using annotated descriptions  
 297 as the learning objective. This allows users to edit videos directly from these descriptions without  
 298 exhaustive analysis. (2) For object insertion, the MLLM provides not only detailed descriptions  
 299 but also frame-wise placement suggestions for new objects, enhancing its utility in video editing  
 300 by avoiding manual trajectory outlining. For training, we convert video object segmentation masks  
 301 into bounding boxes by selecting maximal and minimal coordinates and follow the box planning  
 302 strategy using LLMs (Lin et al., 2023b). We input box coordinates as a sequence of numbers and  
 303 train RACCoN framework to predict these layouts given inpainted videos  $\hat{\mathbf{x}}$ . We perform parameter-  
 304 efficient fine-tuning with LoRA (Hu et al., 2022)<sup>2</sup> on these mixed datasets with CE loss. We freeze  
 305 the visual encoder and LLM backbone, updating the projector, LoRA, and LLM head.

306 **Video Diffusion Model Fine-tuning.** Our video diffusion model builds on the prior image inpainting  
 307 model (Rombach et al., 2022), enhanced with temporal attention layers to capture video dynamics.  
 308 The model is designed to generate video that aligns with input prompts, focusing on object-centric  
 309 video content editing. To support this, we develop a training dataset of mask-object-description  
 310 triples. We use GPT-4 to produce single-object descriptions from long, detailed video narratives,  
 311 framing this task as a multi-choice QA problem. Next, for the three video editing subtasks, we design  
 312 specific input-output combinations: (1) **Video Object Addition**: Inputs: inpainted video  $\hat{\mathbf{x}}$ , object  
 313 bounding boxes from segmentation masks  $m$ , and detailed object description  $p$ . Output: original  
 314 video  $\mathbf{x}$ . (2) **Video Object Removal**: Inputs: original video  $\mathbf{x}$ , object segmentation masks  $m$ , and a  
 315 fixed background prompt. Output: inpainted video  $\hat{\mathbf{x}}$ . (3) **Video Object Change**: Inputs: original  
 316 video  $\mathbf{x}$ , object segmentation masks  $m$ , and object description  $p$ . Output: original video  $\mathbf{x}$ . The  
 317 model is fine-tuned following the prior work (Wu et al., 2023a), updating only the temporal layers  
 318 and the query projections within the self-attention and cross-attention modules. We employ the MSE  
 319 loss between generated and random noise. See Appendix for more details on the dataset and training.

320

## 4 EXPERIMENTAL RESULTS

321

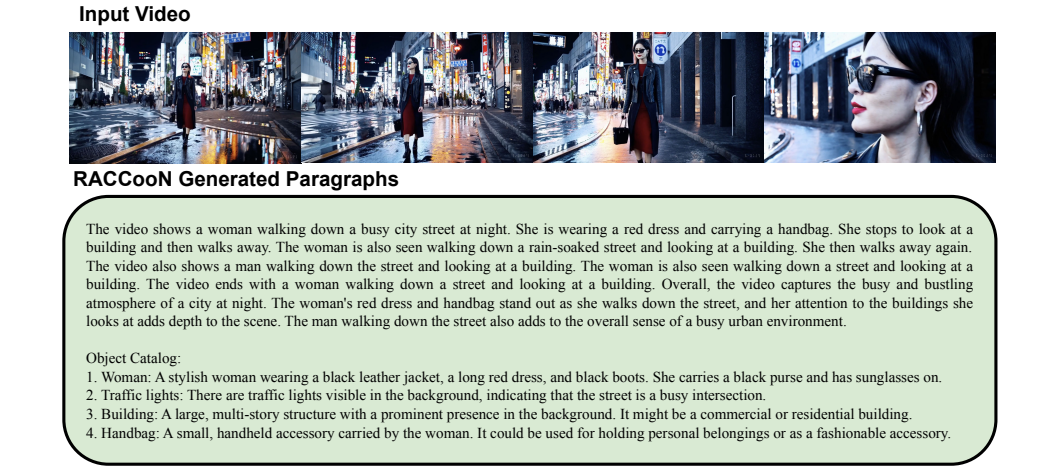
322 **Tasks & Datasets:** We evaluate our RACCoN framework on diverse video datasets across tasks,  
 323 including video captioning (**YouCook2** (Zhou et al., 2018a), **VPLM**), text-based video content editing

---

<sup>2</sup>We employ LoRA for query and value for each self-attention.

324  
325 **Table 1: Results of Single Object Prediction**  
326 on VPLM test set. Metrics are abbreviated:S:  
327 **SPICE**, B: **BLEU-4**, C: **CIDEr**.

Methods	S	B	C	IoU	FVD	CLIP
<i>open-source MLLMs</i>						
LLaVA (Liu et al., 2023b)	17.4	27.5	18.5	-	-	-
Video-Chat (Li et al., 2023)	18.2	25.3	19.1	-	-	-
PG-VL (Munasighe et al., 2023)	18.2	27.4	14.6	-	-	-
<i>proprietary MLLMs</i>						
Gemini 1.5 Pro (Team et al., 2023)	19.2	23.5	11.0	0.115	371.63	0.978
GPT-4o (gpt 4o, 2024)	20.6	28.0	37.4	0.179	447.67	0.977
<b>RACCooN</b>	<b>23.1</b>	<b>31.0</b>	<b>33.5</b>	<b>0.218</b>	<b>432.42</b>	<b>0.983</b>



354 Figure 4: Qualitative V2P example of our RACCooN on Sora video.  
355

356 **(DAVIS (Pont-Tuset et al., 2017), VPLM), and conditional video generation (ActivityNet (Krishna  
357 et al., 2017), YouCook2 (Zhou et al., 2018a), UCF101 (Soomro et al., 2012)).**

358 **Metrics:** For each task, we evaluate our approach with various metrics. **(1) Video Caption:** following  
359 previous works (Yang et al., 2023; Zhou et al., 2018b), we conduct a comprehensive human evaluation  
360 and adopt general metrics for our long video descriptions, including SPICE (Anderson et al., 2016),  
361 BLEU-4 (Vedantam et al., 2015), and CIDEr (Vedantam et al., 2015). **(2) Video Object Layout**  
362 **Planning:** following the prior work (Lin et al., 2023b), we evaluate the framework for object layout  
363 planning by bounding box IoU, FVD (Unterthiner et al., 2019), and CLIP-score (Radford et al.,  
364 2021). **(3) Text-based Video Content Editing:** following prior works (Geyer et al., 2023; Ceylan  
365 et al., 2023; Yang et al., 2024), we evaluate the framework by CLIP-Text, CLIP-Frame, Qedit (Yang  
366 et al., 2024), and SSIM (Hore & Ziou, 2010). **(4) Conditional Video Generation:** we measure  
367 FVD (Unterthiner et al., 2019), CLIP-Score (Radford et al., 2021), and SSIM (Hore & Ziou, 2010).

368 **Implementation Details:** In V2P generation, we set  $k = [20, 25]$  and  $v = [5, 6]$  for superpixel  
369 clustering. We use CLIP-L/14@336 (Radford et al., 2021) as the image encoder and Vicuna-1.5 (Zheng  
370 et al., 2024) as the LLM. Our P2V model is started from StableDiffusion-2.0-Inpainting (Rombach  
371 et al., 2022). We split the VPLM datasets into train and test sets, with the test set containing 50 unique  
372 video-paraphrase pairs (for V2P) and 180 mask-object-description triples (for P2V). We manually  
373 annotate the editing prompts for the object-changing subtask. We quantitatively compare RACCooN  
374 and other baselines on the VLPM test set. To focus on generation results rather than grounding ability,  
375 we apply the same ground truth masks and captions to all methods for P2V evaluation. See the  
376 Appendix for more details on datasets, metrics, implementations, ablations, and qualitative analysis.

#### 377 4.1 VIDEO-TO-PARAGRAPH GENERATION

378 **Video-Paragraph Alignment.** We conducted a quantitative evaluation of our proposed RACCooN  
379 framework’s video-to-paraphrase generation capabilities, comparing it against strong baselines with a  
380 focus on object-centric captioning and object layout planning. The results, summarized in Tab. 1,  
381 show that open-source video-LLMs (e.g., PG-VL, Video-Chat) which have smaller LLMs (< 13B

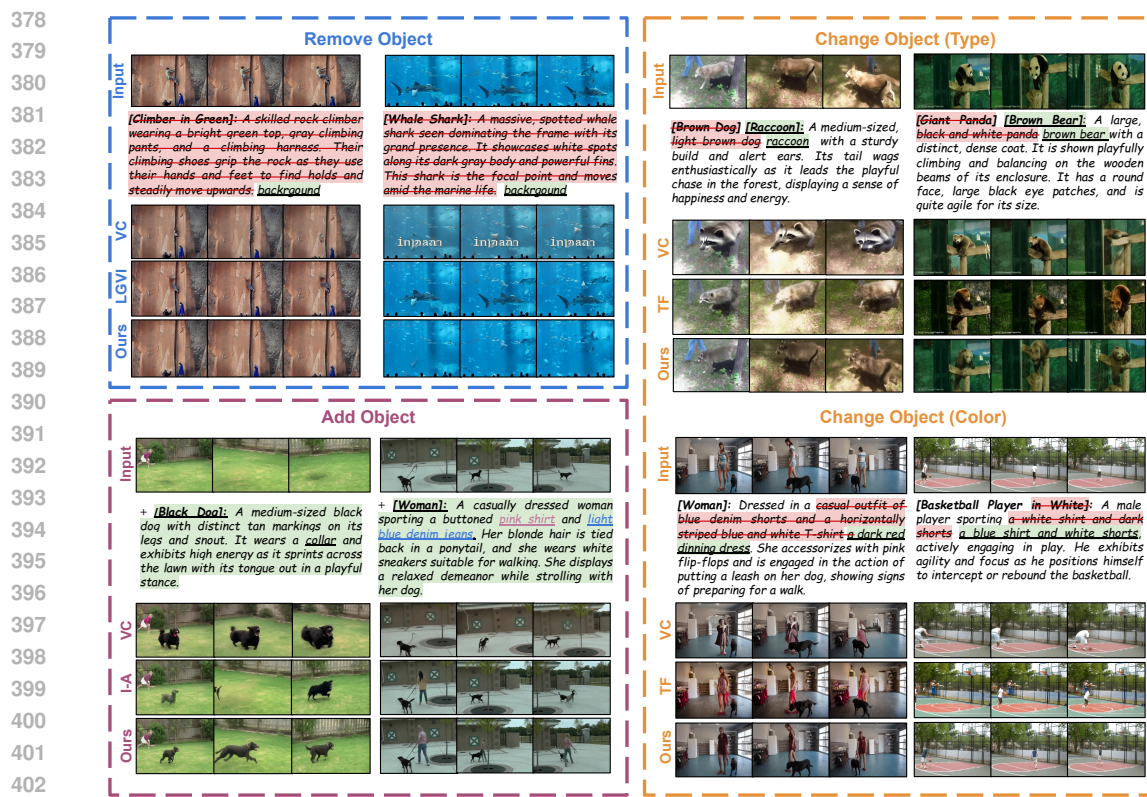


Figure 5: **Qualitative Comparison between RACCoN and other baselines.** Baseline names are abbreviated: **VC**: VideoComposer, **I-A**: Inpainting Anything, **TF**: TokenFlow. We underline visual details in our caption. More visualizations are in Appendix.

Table 3: **Results of Video Content Editing on three sub-tasks** on VPLM test. We gray out models that conduct the DDIM inversion process and have a different focus on our inpainting-based model.

Model	Change Object			Remove Object			Add Object		
	CLIP-T↑	CLIP-F↑	Qedit↑	FVD↓	SSIM↑	PSNR↑	FVD↓	SSIM↑	PSNR↑
<i>Inversion-based Models</i>									
LOVECon (Liao & Deng, 2023)	29.36	94.77	1.29	1319.51	60.40	17.78	1433.12	58.51	17.35
FateZero (Qi et al., 2023)	25.18	94.47	1.01	1037.05	47.35	15.16	1474.80	47.65	15.45
TokenFlow (Geyer et al., 2023)	29.25	96.23	1.31	1317.29	47.06	15.83	1373.20	49.95	15.95
<i>Inpainting-Based Models</i>									
Inpaint Anything (Yu et al., 2023)	24.86	92.01	1.01	383.81	82.33	27.69	712.59	77.75	22.41
LGV1 (Wu et al., 2024)	23.82	<b>95.33</b>	1.04	915.24	56.16	19.14	1445.43	47.93	16.09
VideoComposer (Wang et al., 2024b)	27.61	94.18	<b>1.25</b>	827.04	47.34	17.55	1151.90	48.01	15.76
PGVL + SD-v2.0-inpainting	24.01	90.11	1.01	282.31	82.33	27.69	1579.65	43.21	15.76
<b>RACCoN</b>	<b>27.85</b>	<b>94.78</b>	<u>1.15</u>	<b>162.03</b>	<b>84.38</b>	<b>30.34</b>	<b>415.82</b>	<b>77.81</b>	<b>23.38</b>

parameters), struggle with object-centric captioning and usually fail to generate layout planning. This is primarily due to their lack of instructional fine-tuning and insufficient video detail modeling without multi-granular pooling. In contrast, our RACCoN framework demonstrates superior performance in both object-centric captioning and complex object layout planning, benefiting from the instructional tuning on our VPLM dataset. Additionally, our method achieves competitive performance with proprietary MLLMs (e.g., Gemini 1.5 Pro, GPT-4o) in key object captioning and layout planning, demonstrating its superior instruction following and generation quality. **Human Evaluation & Qualitative Examples.** We conducted a human evaluation to compare our auto-generated captions with those from a strong baseline and human annotations on ten randomly selected YouCook2 videos (each three to five minutes long with multiple scenes and complex viewpoints). Five evaluators rated these based on Logic Fluency, Language Fluency, Video Summary, and Video Details (details in Appendix). The average scores for each criterion and their overall mean are illustrated in Tab. 2. Our method significantly surpassed both the PG-VL-generated and ground truth captions in all metrics,

432 showing a **4.9%<sub>p</sub>** and **21.8%<sub>p</sub>** **absolute improvement** respectively, and matched the ground truth  
 433 in capturing *Video Details* with a **9.4%<sub>p</sub>** enhancement over the baseline, highlighting RACCoON’s  
 434 superior capability in capturing video details. We additionally visualize descriptions generated by  
 435 our RACCoON. We use a well-known generated video from the Sora ([openai, 2024](#)) generated demo  
 436 example. As shown in Fig. 4, it demonstrates our model’s robust capability to auto-describe complex  
 437 video content without human textual input.

438

## 439 4.2 INSTRUCTIONAL VIDEO EDITING WITH RACCOON

440

441 **Quantitative Evaluation.** As shown in Tab. 3, we quantitatively compare the video editing ability of  
 442 RACCoON with strong video editing models based on inpainting or DDIM-inversion ([Hertz et al.,](#)  
 443 [2022](#)) across three object-centric video content editing subtasks: *object changing, removal, and*  
 444 *adding*. In general, RACCoON outperforms all baselines across 9 metrics. For object changing,  
 445 RACCoON outperforms the best-performing baseline by 0.8% on CLIP-T, indicating better video-text  
 446 alignment while maintaining temporal consistency, as demonstrated by comparable CLIP-F and  
 447 Qedit scores. Note that LGVI is not designed to alter video attributes and tends to preserve video  
 448 content with marginal change (i.e., identical input and output videos), resulting in improved CLIP-F  
 449 scores. In the object removal task, RACCoON shows significant improvements over strong baselines  
 450 (relatively +57.8% FVD, +2.5% SSIM, +9.6% PSNR). Such improvements are maintained in the  
 451 addition task (relatively +41.6% FVD, +4.3% PSNR). Meanwhile, some DDIM inversion-based  
 452 models (e.g., TokenFlow ([Geyer et al., 2023](#))) work well for specific tasks (change objects), but do  
 453 not handle other types of editing. In contrast, our method is an all-rounder player.

454

We further emphasize that **a simple combination of existing models cannot achieve an effective framework**, leading to inferior instruction-following and editing abilities. This is evident in the degraded performance of open-source Video-LLM baselines (Tabs. 1 and 2) and other video editing models (Tab. 3). To address these limitations, we made unique novelty in technical and dataset contributions and achieved significant improvements in both video understanding and editing. This is evident in the comparison of our RACCoON with a multi-agent baseline combining a powerful open-source video reasoning framework and video diffusion models (PG-Video-LLaMA + StableDiffusion 2.0-inpainting) in Tab. 3. RACCoON outperforms the *PGVL + SD 2.0-inpainting* by a significant margin across all metrics and editing tasks, highlighting the effectiveness of our proposed framework.

462

**Visualization.** In Fig. 5, we compare videos generated by RACCoON with several SoTA baselines across three video content editing tasks. For object removal, RACCoON demonstrates superior results, naturally and smoothly inpainting the background, whereas VideoComposer generates unexpected content and LGVI fails to accurately remove objects across frames. For object addition, compared to Inpainting-Anything and VideoComposer, which often miss objects or produce distorted generations, RACCoON generates objects with more fluent and natural motion, accurately reflecting caption details (e.g., the *collar* of the dog, the *pink shirt*, and *blue jeans* for the woman). For changing objects, our method outperforms inpainting-based VideoComposer and inversion-based TokenFlow. RACCoON accurately re-paints objects to achieve object editing for color (*white*→*blue*) and type (*dog*→*RACCoON*), while others struggle to meet requirements.

471

**Ablation Studies.** As shown in Tab. 4, we further validate the effectiveness of components by replacing detailed descriptions with short captions, and oracle masks/planning boxes with model-generated ones. In adding objects, our detailed object descriptions can benefit generation by providing accurate details, leading to improved quantitative results (relatively +14.4% FVD). We further replace GT boxes with boxes predicted by RACCoON, and still show superior performance over other baseline methods with oracle boxes in Tab. 3. It demonstrates that our V2P stage can thus automatically generate planning from a given video to eliminate users’ labor. Next, in object removal and changing, we replace the oracle masks with grounding ([Liu et al., 2023d](#)) and tracking ([Cheng et al., 2023](#)) tools generated mask,

Table 4: **Ablation on video object changing, removing, and adding** with different inputs.

Settings	FVD↓	SSIM↑	PSNR↑
<i>add object</i>			
RACCoON	415.80	77.81	23.38
w/o detail caption	476.01	76.80	23.14
w/o oracle planning	969.95	76.65	21.21
<i>remove object</i>			
RACCoON	162.03	84.38	30.34
w/o oracle mask	398.01	81.60	27.15
Setting	CLIP-T	CLIP-F	Qedit
<i>change object</i>			
RACCoON	27.85	94.78	1.15
w/o oracle mask	27.23	94.33	1.14

486  
 487 **Table 5: Results of Inversion-based Video Editing** on DAVIS Video. Our generated paragraph  
 488 can be integrated with different SoTA inversion-based video editing models (e.g. TokenFlow or  
 489 Fate-Zero). *attr.* and *ins.* indicate *attribute-level* and *instance-level* editing.  
 490

Model	CLIP-Text			CLIP-Frame			SSIM		
	attr.	ins.	all	attr.	ins.	all	attr.	ins.	all
FateZero (Qi et al., 2023)	28.9	27.2	28.1	<b>95.6</b>	<b>95.1</b>	<b>95.3</b>	71.5	70.8	71.2
FateZero (Qi et al., 2023) + RACCoN	<b>31.7</b>	<b>30.7</b>	<b>31.2</b>	95.5	<b>95.1</b>	<b>95.3</b>	<b>72.1</b>	<b>72.3</b>	<b>72.2</b>
TokenFlow (Geyer et al., 2023)	31.4	29.8	30.6	94.6	94.1	94.3	57.0	56.0	56.5
TokenFlow (Geyer et al., 2023) + RACCoN	<b>32.6</b>	<b>31.6</b>	<b>32.1</b>	<b>94.7</b>	<b>94.3</b>	<b>94.5</b>	<b>58.0</b>	<b>57.3</b>	<b>57.6</b>

496  
 497 **Table 6: Results of Conditional Video Generation** on three datasets. RACCoN framework can be  
 498 integrated with different video generation models (e.g. VideoCrafter or DynamiCrafter).

Model	ActivityNet			YouCook2			UCF101		
	FVD↓	CLIP↑	SSIM↑	FVD↓	CLIP↑	SSIM↑	FVD↓	CLIP↑	SSIM↑
VideoCrafter (Chen et al., 2023)	3743.62	9.58	22.26	4731.22	<b>9.89</b>	20.58	3556.06	<b>9.81</b>	18.32
VideoCrafter (Chen et al., 2023) + RACCoN	<b>2357.41</b>	<b>10.53</b>	<b>24.02</b>	<b>3046.82</b>	9.47	<b>23.89</b>	<b>2208.90</b>	9.60	<b>22.32</b>
DynamiCrafter (Xing et al., 2023)	1632.30	10.65	32.46	2059.93	<b>11.95</b>	37.22	1588.57	<b>11.98</b>	38.81
DynamiCrafter (Xing et al., 2023) + RACCoN	<b>1536.63</b>	<b>10.69</b>	<b>32.86</b>	<b>1904.08</b>	10.03	<b>38.78</b>	<b>1573.27</b>	9.76	<b>39.83</b>

504 it shows marginally decrement for changing objects, and our framework still shows strong results  
 505 over other baselines in Tab. 3 with oracle masks. It suggests that RACCoN is effective and robust  
 506 to handle diverse editing skills in a non-orcale setting (See the Appendix).

#### 508 4.3 ENHANCING INVERSION-BASED VIDEO EDITING & GENERATION WITH RACCOON

510 We further validate that detailed paragraphs can benefit video generative tasks (e.g., inversion-based  
 511 video editing and video generation). Our RACCoN captions can be integrated with off-shelf SoTA  
 512 video editing and generation models to enhance them. See Appendix for more details.

514 **Inversion-based Video Editing.** Our RACCoN framework can significantly enhance video editing  
 515 tasks. We integrated it into two SoTA methods, TokenFlow (Geyer et al., 2023) and FateZero (Qi et al.,  
 516 2023), and compared their performance with different text inputs. The baseline used human-written  
 517 short captions, while *baseline*+RACCoN used generated detailed captions. As shown in Tab. 5,  
 518 integrating RACCoN significantly improved performance. FateZero+RACCoN achieved an 11.0%  
 519 and 1.4% relative increase in CLIP-Text and SSIM scores, respectively. TokenFlow+RACCoN  
 520 saw increases of 4.9% and 1.9%. These results indicate that detailed captions enhance text-to-video  
 521 alignment and localized editing, while preserving temporal consistency and quality.

522 **Conditional Video Generation.** We also integrated RACCoN with various SoTA video gener-  
 523 ation methods, such as VideoCrafter (Chen et al., 2023) and DynamiCrafter (Xing et al., 2023).  
 524 VideoCrafter was tested in a Text-to-Video setting, while DynamiCrafter was in an Image-Text-  
 525 to-Video setting. We evaluated our framework on ActivityNet, YouCook2, and UCF101 datasets.  
 526 As listed in Tab. 6, VideoCrafter’s generated videos often failed to align with the GT captions,  
 527 especially in complex videos. In contrast, our framework improved video quality and alignment with  
 528 auto-generated detailed paragraphs, achieving substantial improvements of 36.9% in FVD and 15.3%  
 529 in SSIM. We noted consistent improvements in FVD, CLIP, and SSIM scores with RACCoN. It  
 530 underscores our effectiveness in augmenting video generation models with automated descriptions.

## 531 5 CONCLUSION

533 Our proposed RACCoN framework newly introduces an auto-descriptive video-to-paragraph-to-  
 534 video generative framework. RACCoN automatically generates video descriptions by leveraging a  
 535 multi-granular spatiotemporal pooling strategy, enhancing the model’s ability to recognize detailed,  
 536 localized video information. RACCoN then uses these enriched descriptions to edit and generate  
 537 video content, offering users the flexibility to modify content through textual updates, thus eliminating  
 538 the need for detailed video annotations. These video editing and generation abilities of RACCoN  
 539 framework highlight notable effectiveness and enable a broader range of users to engage in video  
 creation and editing tasks without the faithfully written textual prompts.

540           **ETHICS STATEMENT**  
 541

542       The performance of our proposed framework in paragraph generation, video generation, and editing  
 543       is influenced by the employed pre-trained backbones, including an LLM (Touvron et al., 2023).  
 544       LLM-empowered video description and photorealistic video creation/editing inherit biases from  
 545       their training data, leading to several potentially negative impacts, including societal stereotypes,  
 546       biased interpretation of actions, and privacy concerns. To mitigate these potential negative impacts,  
 547       it is essential to carefully develop and implement generative and video description models, such as  
 548       considering diversifying training datasets, implementing fairness and bias evaluation metrics, and  
 549       engaging communities to understand and address their concerns.

550  
 551           **REPRODUCIBILITY STATEMENT**  
 552

553       This paper fully discloses all the information needed to reproduce the main experimental results of  
 554       the paper to the extent that it affects the main claims and/or conclusions. To maximize reproducibility,  
 555       we have included our code in the supplementary material. Also, we report all of our hyperparameter  
 556       settings and model details in the Appendix.

557  
 558           **REFERENCES**  
 559

- 560       Josh Achiam, Steven Adler, Sandhini Agarwal, Lama Ahmad, Ilge Akkaya, Florencia Leoni Aleman,  
 561       Diogo Almeida, Janko Altenschmidt, Sam Altman, Shyamal Anadkat, et al. Gpt-4 technical report.  
 562       *arXiv preprint arXiv:2303.08774*, 2023.
- 563       Peter Anderson, Basura Fernando, Mark Johnson, and Stephen Gould. Spice: Semantic propositional  
 564       image caption evaluation. In *Computer Vision–ECCV 2016: 14th European Conference, Amsterdam, The Netherlands, October 11–14, 2016, Proceedings, Part V 14*, pp. 382–398. Springer,  
 565       2016.
- 566       Max Bain, Arsha Nagrani, Gü̈l Varol, and Andrew Zisserman. Frozen in time: A joint video and  
 567       image encoder for end-to-end retrieval. In *Proceedings of the IEEE/CVF International Conference  
 568       on Computer Vision*, pp. 1728–1738, 2021.
- 569       Andreas Blattmann, Tim Dockhorn, Sumith Kulal, Daniel Mendelevitch, Maciej Kilian, Dominik  
 570       Lorenz, Yam Levi, Zion English, Vikram Voleti, Adam Letts, et al. Stable video diffusion: Scaling  
 571       latent video diffusion models to large datasets. *arXiv preprint arXiv:2311.15127*, 2023.
- 572       Duygu Ceylan, Chun-Hao P Huang, and Niloy J Mitra. Pix2video: Video editing using image  
 573       diffusion. In *Proceedings of the International Conference on Computer Vision (ICCV)*, 2023.
- 574       Wenhao Chai, Xun Guo, Gaoang Wang, and Yan Lu. Stablevideo: Text-driven consistency-aware  
 575       diffusion video editing. In *Proceedings of the International Conference on Computer Vision  
 576       (ICCV)*, 2023.
- 577       Haoxin Chen, Menghan Xia, Yingqing He, Yong Zhang, Xiaodong Cun, Shaoshu Yang, Jinbo  
 578       Xing, Yaofang Liu, Qifeng Chen, Xintao Wang, et al. Videocrafter1: Open diffusion models for  
 579       high-quality video generation. *arXiv preprint arXiv:2310.19512*, 2023.
- 580       Yangming Cheng, Liulei Li, Yuanyou Xu, Xiaodi Li, Zongxin Yang, Wenguan Wang, and Yi Yang.  
 581       Segment and track anything. *arXiv preprint arXiv:2305.06558*, 2023.
- 582       Guillaume Cleuziou. A generalization of k-means for overlapping clustering. *Rapport technique*,  
 583       2007.
- 584       Paul Couairon, Clément Rambour, Jean-Emmanuel Haugéard, and Nicolas Thome. Videdit: Zero-shot  
 585       and spatially aware text-driven video editing. *arXiv preprint arXiv:2306.08707*, 2023.
- 586       Patrick Esser, Johnathan Chiu, Parmida Atighehchian, Jonathan Granskog, and Anastasis Germanidis.  
 587       Structure and content-guided video synthesis with diffusion models. In *Proceedings of the  
 588       International Conference on Computer Vision (ICCV)*, 2023.

- 594 Quanfu Fan, Rameswar Panda, et al. An image classifier can suffice for video understanding. *arXiv*  
 595 *preprint arXiv:2106.14104*, 2, 2021.  
 596
- 597 Xiang Fan, Anand Bhattad, and Ranjay Krishna. Videoshop: Localized semantic video editing with  
 598 noise-extrapolated diffusion inversion. *arXiv preprint arXiv:2403.14617*, 2024.
- 599 Kirill Gavrilyuk, Amir Ghodrati, Zhenyang Li, and Cees GM Snoek. Actor and action video  
 600 segmentation from a sentence. In *Proceedings of the IEEE conference on computer vision and*  
 601 *pattern recognition*, pp. 5958–5966, 2018.
- 602 Michal Geyer, Omer Bar-Tal, Shai Bagon, and Tali Dekel. Tokenflow: Consistent diffusion features  
 603 for consistent video editing. *arXiv preprint arXiv:2307.10373*, 2023.
- 604 Daniela Giordano, Francesca Murabito, Simone Palazzo, and Concetto Spampinato. Superpixel-based  
 605 video object segmentation using perceptual organization and location prior. In *Proceedings of the*  
 606 *IEEE International Conference on Computer Vision and Pattern Recognition (CVPR)*, 2015.
- 607 gpt 4o. <https://openai.com/index/hello-gpt-4o/>. May 2024.
- 608 Amir Hertz, Ron Mokady, Jay Tenenbaum, Kfir Aberman, Yael Pritch, and Daniel Cohen-Or. Prompt-  
 609 to-prompt image editing with cross attention control. *arXiv preprint arXiv:2208.01626*, 2022.
- 610 Wenyi Hong, Ming Ding, Wendi Zheng, Xinghan Liu, and Jie Tang. Cogvideo: Large-scale  
 611 pretraining for text-to-video generation via transformers. *arXiv preprint arXiv:2205.15868*, 2022.
- 612 Alain Hore and Djemel Ziou. Image quality metrics: Psnr vs. ssim. In *2010 20th international*  
 613 *conference on pattern recognition*, pp. 2366–2369. IEEE, 2010.
- 614 Edward J Hu, Yelong Shen, Phillip Wallis, Zeyuan Allen-Zhu, Yuanzhi Li, Shean Wang, Lu Wang,  
 615 and Weizhu Chen. Lora: Low-rank adaptation of large language models. In *Proceedings of the*  
 616 *International Conference on Learning Representations (ICLR)*, 2022.
- 617 Eddy Ilg, Nikolaus Mayer, Tonmoy Saikia, Margret Keuper, Alexey Dosovitskiy, and Thomas Brox.  
 618 Flownet 2.0: Evolution of optical flow estimation with deep networks. In *Proceedings of the IEEE*  
 619 *conference on computer vision and pattern recognition*, pp. 2462–2470, 2017.
- 620 Hyeonho Jeong and Jong Chul Ye. Ground-a-video: Zero-shot grounded video editing using text-to-  
 621 image diffusion models. *arXiv preprint arXiv:2310.01107*, 2023.
- 622 Yongrae Jo, Seongyun Lee, Aiden SJ Lee, Hyunji Lee, Hanseok Oh, and Minjoon Seo. Zero-shot  
 623 dense video captioning by jointly optimizing text and moment. *arXiv preprint arXiv:2307.02682*,  
 624 2023.
- 625 Tsung-Wei Ke, Sangwoo Mo, and X Yu Stella. Learning hierarchical image segmentation for  
 626 recognition and by recognition. In *Proceedings of the International Conference on Learning*  
 627 *Representations (ICLR)*, 2023.
- 628 Sina Khanmohammadi, Naiier Adibeig, and Samaneh Shanehbandy. An improved overlapping  
 629 k-means clustering method for medical applications. *Expert Systems with Applications*, 2017.
- 630 Diederik P Kingma and Max Welling. Auto-encoding variational bayes. *arXiv preprint*  
 631 *arXiv:1312.6114*, 2013.
- 632 Alexander Kirillov, Eric Mintun, Nikhila Ravi, Hanzi Mao, Chloe Rolland, Laura Gustafson, Tete  
 633 Xiao, Spencer Whitehead, Alexander C. Berg, Wan-Yen Lo, Piotr Dollár, and Ross Girshick.  
 634 Segment anything. *arXiv:2304.02643*, 2023.
- 635 Dan Kondratyuk, Lijun Yu, Xiuye Gu, José Lezama, Jonathan Huang, Rachel Hornung, Hartwig  
 636 Adam, Hassan Akbari, Yair Alon, Vighnesh Birodkar, et al. Videopoet: A large language model  
 637 for zero-shot video generation. *arXiv preprint arXiv:2312.14125*, 2023.
- 638 Ranjay Krishna, Kenji Hata, Frederic Ren, Li Fei-Fei, and Juan Carlos Niebles. Dense-captioning  
 639 events in videos. In *Proceedings of the IEEE international conference on computer vision*, pp.  
 640 706–715, 2017.

- 648 KunChang Li, Yinan He, Yi Wang, Yizhuo Li, Wenhui Wang, Ping Luo, Yali Wang, Limin Wang, and  
 649 Yu Qiao. Videochat: Chat-centric video understanding. *arXiv preprint arXiv:2305.06355*, 2023.  
 650
- 651 Zhengqin Li and Jiansheng Chen. Superpixel segmentation using linear spectral clustering. In  
 652 *Proceedings of the IEEE International Conference on Computer Vision and Pattern Recognition*  
 653 (*CVPR*), 2015.
- 654 Zhenyi Liao and Zhijie Deng. Lovecon: Text-driven training-free long video editing with controlnet.  
 655 *arXiv preprint arXiv:2310.09711*, 2023.  
 656
- 657 Bin Lin, Bin Zhu, Yang Ye, Munan Ning, Peng Jin, and Li Yuan. Video-llava: Learning united visual  
 658 representation by alignment before projection. *arXiv preprint arXiv:2311.10122*, 2023a.
- 659 Han Lin, Abhay Zala, Jaemin Cho, and Mohit Bansal. Videodirectorgpt: Consistent multi-scene  
 660 video generation via llm-guided planning. *arXiv preprint arXiv:2309.15091*, 2023b.  
 661
- 662 Fuxiao Liu, Kevin Lin, Linjie Li, Jianfeng Wang, Yaser Yacoob, and Lijuan Wang. Mitigating  
 663 hallucination in large multi-modal models via robust instruction tuning. In *Proceedings of the*  
 664 *International Conference on Learning Representations (ICLR)*, 2023a.
- 665 Haotian Liu, Chunyuan Li, Qingyang Wu, and Yong Jae Lee. Visual instruction tuning. In *Advances*  
 666 *in Neural Information Processing Systems (NeurIPS)*, 2023b.  
 667
- 668 Shaoteng Liu, Yuechen Zhang, Wenbo Li, Zhe Lin, and Jiaya Jia. Video-p2p: Video editing with  
 669 cross-attention control. *arXiv preprint arXiv:2303.04761*, 2023c.  
 670
- 671 Shilong Liu, Zhaoyang Zeng, Tianhe Ren, Feng Li, Hao Zhang, Jie Yang, Chunyuan Li, Jianwei  
 672 Yang, Hang Su, Jun Zhu, et al. Grounding dino: Marrying dino with grounded pre-training for  
 673 open-set object detection. *arXiv preprint arXiv:2303.05499*, 2023d.  
 674
- 675 Ziqiao Ma, Jiayi Pan, and Joyce Chai. World-to-words: Grounded open vocabulary acquisition  
 676 through fast mapping in vision-language models. *arXiv preprint arXiv:2306.08685*, 2023.  
 677
- 678 Arjun Majumdar, Ayush Shrivastava, Stefan Lee, Peter Anderson, Devi Parikh, and Dhruv Batra.  
 679 Improving vision-and-language navigation with image-text pairs from the web. In *Computer*  
 680 *Vision–ECCV 2020: 16th European Conference, Glasgow, UK, August 23–28, 2020, Proceedings,*  
 681 *Part VI 16*, pp. 259–274. Springer, 2020.  
 682
- 683 Kangfu Mei and Vishal Patel. Vidm: Video implicit diffusion models. In *Proceedings of the AAAI*  
 684 *National Conference on Artificial Intelligence (AAAI)*, 2023.  
 685
- 686 Shehan Munasinghe, Rusiru Thushara, Muhammad Maaz, Hanoona Abdul Rasheed, Salman Khan,  
 687 Mubarak Shah, and Fahad Khan. Pg-video-llava: Pixel grounding large video-language models.  
 688 *arXiv preprint arXiv:2311.13435*, 2023.  
 689
- 690 openai. <https://openai.com/sora>. 2024.  
 691
- 692 Jordi Pont-Tuset, Federico Perazzi, Sergi Caelles, Pablo Arbeláez, Alex Sorkine-Hornung, and  
 693 Luc Van Gool. The 2017 davis challenge on video object segmentation. *arXiv preprint*  
 694 *arXiv:1704.00675*, 2017.  
 695
- 696 Chenyang Qi, Xiaodong Cun, Yong Zhang, Chenyang Lei, Xintao Wang, Ying Shan, and Qifeng Chen.  
 697 Fatezero: Fusing attentions for zero-shot text-based video editing. *arXiv preprint arXiv:2303.09535*,  
 698 2023.  
 699
- 700 Alec Radford, Jong Wook Kim, Chris Hallacy, Aditya Ramesh, Gabriel Goh, Sandhini Agarwal,  
 701 Girish Sastry, Amanda Askell, Pamela Mishkin, Jack Clark, et al. Learning transferable visual  
 702 models from natural language supervision. In *Proceedings of the International Conference on*  
 703 *Machine Learning (ICML)*, 2021.  
 704
- 705 Tianhe Ren, Shilong Liu, Ailing Zeng, Jing Lin, Kunchang Li, He Cao, Jiayu Chen, Xinyu Huang,  
 706 Yukang Chen, Feng Yan, Zhaoyang Zeng, Hao Zhang, Feng Li, Jie Yang, Hongyang Li, Qing  
 707 Jiang, and Lei Zhang. Grounded sam: Assembling open-world models for diverse visual tasks.  
 708 *arXiv preprint arXiv:2401.14159*, 2024.  
 709

- 702 Robin Rombach, Andreas Blattmann, Dominik Lorenz, Patrick Esser, and Björn Ommer. High-  
 703 resolution image synthesis with latent diffusion models. In *Proceedings of the IEEE/CVF confer-  
 704 ence on computer vision and pattern recognition*, pp. 10684–10695, 2022.
- 705
- 706 Zhiqiang Shen, Jianguo Li, Zhou Su, Minjun Li, Yurong Chen, Yu-Gang Jiang, and Xiangyang Xue.  
 707 Weakly supervised dense video captioning. In *Proceedings of the IEEE Conference on Computer  
 708 Vision and Pattern Recognition*, pp. 1916–1924, 2017.
- 709
- 710 Khurram Soomro, Amir Roshan Zamir, and Mubarak Shah. Ucf101: A dataset of 101 human actions  
 711 classes from videos in the wild. *arXiv preprint arXiv:1212.0402*, 2012.
- 712
- 713 Gemini Team, Rohan Anil, Sebastian Borgeaud, Yonghui Wu, Jean-Baptiste Alayrac, Jiahui Yu, Radu  
 714 Soricut, Johan Schalkwyk, Andrew M Dai, Anja Hauth, et al. Gemini: a family of highly capable  
 715 multimodal models. *arXiv preprint arXiv:2312.11805*, 2023.
- 716
- 717 Yoad Tewel, Yoav Shalev, Roy Nadler, Idan Schwartz, and Lior Wolf. Zero-shot video captioning  
 718 with evolving pseudo-tokens. *arXiv preprint arXiv:2207.11100*, 2022.
- 719
- 720 Hugo Touvron, Louis Martin, Kevin Stone, Peter Albert, Amjad Almahairi, Yasmine Babaei, Nikolay  
 721 Bashlykov, Soumya Batra, Prajjwal Bhargava, Shruti Bhosale, et al. Llama 2: Open foundation  
 722 and fine-tuned chat models. *arXiv preprint arXiv:2307.09288*, 2023.
- 723
- 724 Thomas Unterthiner, Sjoerd van Steenkiste, Karol Kurach, Raphaël Marinier, Marcin Michalski, and  
 725 Sylvain Gelly. Fvd: A new metric for video generation. In *ICLR workshop*, 2019.
- 726
- 727 Ramakrishna Vedantam, C Lawrence Zitnick, and Devi Parikh. Cider: Consensus-based image  
 728 description evaluation. In *Proceedings of the IEEE conference on computer vision and pattern  
 729 recognition*, pp. 4566–4575, 2015.
- 730
- 731 Bairui Wang, Lin Ma, Wei Zhang, and Wei Liu. Reconstruction network for video captioning. In  
 732 *Proceedings of the IEEE International Conference on Computer Vision and Pattern Recognition  
 733 (CVPR)*, 2018.
- 734
- 735 Lei Wang, Jiabang He, Shenshen Li, Ning Liu, and Ee-Peng Lim. Mitigating fine-grained hallucina-  
 736 tion by fine-tuning large vision-language models with caption rewrites. In *International Conference  
 737 on Multimedia Modeling*. Springer, 2024a.
- 738
- 739 Teng Wang, Ruimao Zhang, Zhichao Lu, Feng Zheng, Ran Cheng, and Ping Luo. End-to-end dense  
 740 video captioning with parallel decoding. In *Proceedings of the IEEE/CVF International Conference  
 741 on Computer Vision*, pp. 6847–6857, 2021.
- 742
- 743 Wen Wang, Yan Jiang, Kangyang Xie, Zide Liu, Hao Chen, Yue Cao, Xinlong Wang, and Chun-  
 744 hua Shen. Zero-shot video editing using off-the-shelf image diffusion models. *arXiv preprint  
 745 arXiv:2303.17599*, 2023.
- 746
- 747 Xiang Wang, Hangjie Yuan, Shiwei Zhang, Dayou Chen, Jiuniu Wang, Yingya Zhang, Yujun Shen,  
 748 Deli Zhao, and Jingren Zhou. Videocomposer: Compositional video synthesis with motion  
 749 controllability. *Advances in Neural Information Processing Systems*, 36, 2024b.
- 750
- 751 Joyce Jiyoung Whang, Inderjit S Dhillon, and David F Gleich. Non-exhaustive, overlapping k-means.  
 752 In *Proceedings of the 2015 SIAM international conference on data mining*, pp. 936–944. SIAM,  
 753 2015.
- 754
- 755 Jay Zhangjie Wu, Yixiao Ge, Xintao Wang, Stan Weixian Lei, Yuchao Gu, Yufei Shi, Wynne Hsu,  
 756 Ying Shan, Xiaohu Qie, and Mike Zheng Shou. Tune-a-video: One-shot tuning of image diffusion  
 757 models for text-to-video generation. In *Proceedings of the International Conference on Computer  
 758 Vision (ICCV)*, 2023a.
- Jianzong Wu, Xiangtai Li, Chenyang Si, Shangchen Zhou, Jingkang Yang, Jiangning Zhang, Yining  
 Li, Kai Chen, Yunhai Tong, Ziwei Liu, et al. Towards language-driven video inpainting via  
 multilingual large language models. *arXiv preprint arXiv:2401.10226*, 2024.

- 756 Wenhao Wu, Haipeng Luo, Bo Fang, Jingdong Wang, and Wanli Ouyang. Cap4video: What can  
 757 auxiliary captions do for text-video retrieval? In *Proceedings of the IEEE International Conference*  
 758 *on Computer Vision and Pattern Recognition (CVPR)*, 2023b.
- 759 Shaoan Xie, Zhifei Zhang, Zhe Lin, Tobias Hinz, and Kun Zhang. Smartbrush: Text and shape guided  
 760 object inpainting with diffusion model. In *Proceedings of the IEEE/CVF Conference on Computer*  
 761 *Vision and Pattern Recognition*, pp. 22428–22437, 2023.
- 762 Jinbo Xing, Menghan Xia, Yong Zhang, Haoxin Chen, Xintao Wang, Tien-Tsin Wong, and Ying  
 763 Shan. Dynamicrafter: Animating open-domain images with video diffusion priors. *arXiv preprint*  
 764 *arXiv:2310.12190*, 2023.
- 765 Wilson Yan, Yunzhi Zhang, Pieter Abbeel, and Aravind Srinivas. Videogpt: Video generation using  
 766 vq-vae and transformers. *arXiv preprint arXiv:2104.10157*, 2021.
- 767 Antoine Yang, Arsha Nagrani, Paul Hongseok Seo, Antoine Miech, Jordi Pont-Tuset, Ivan Laptev,  
 768 Josef Sivic, and Cordelia Schmid. Vid2seq: Large-scale pretraining of a visual language model for  
 769 dense video captioning. In *Proceedings of the IEEE International Conference on Computer Vision*  
 770 *and Pattern Recognition (CVPR)*, 2023.
- 771 Fengting Yang, Qian Sun, Hailin Jin, and Zihan Zhou. Superpixel segmentation with fully convolutional  
 772 networks. In *Proceedings of the IEEE International Conference on Computer Vision and*  
 773 *Pattern Recognition (CVPR)*, 2020.
- 774 Xiangpeng Yang, Linchao Zhu, Hehe Fan, and Yi Yang. Eva: Zero-shot accurate attributes and  
 775 multi-object video editing. *arXiv preprint arXiv:2403.16111*, 2024.
- 776 Zongxin Yang and Yi Yang. Decoupling features in hierarchical propagation for video object  
 777 segmentation. In *Advances in Neural Information Processing Systems (NeurIPS)*, 2022.
- 778 Zongxin Yang, Yunchao Wei, and Yi Yang. Associating objects with transformers for video object  
 779 segmentation. In *Advances in Neural Information Processing Systems (NeurIPS)*, 2021.
- 780 Shoubin Yu, Jaehong Yoon, and Mohit Bansal. Crema: Multimodal compositional video reasoning  
 781 via efficient modular adaptation and fusion. *arXiv preprint arXiv:2402.05889*, 2024.
- 782 Tao Yu, Runseng Feng, Ruoyu Feng, Jinming Liu, Xin Jin, Wenjun Zeng, and Zhibo Chen. Inpaint  
 783 anything: Segment anything meets image inpainting. *arXiv preprint arXiv:2304.06790*, 2023.
- 784 Hang Zhang, Xin Li, and Lidong Bing. Video-llama: An instruction-tuned audio-visual language  
 785 model for video understanding. In *Proceedings of the Conference on Empirical Methods in Natural*  
 786 *Language Processing (EMNLP)*, 2023a.
- 787 Yuanhan Zhang, Bo Li, haotian Liu, Yong jae Lee, Liangke Gui, Di Fu, Jiashi Feng, Ziwei Liu, and  
 788 Chunyuan Li. Llava-next: A strong zero-shot video understanding model. <https://llava-vl.github.io/blog/2024-04-30-llava-next-video/>. April 2024.
- 789 Zhixing Zhang, Bichen Wu, Xiaoyan Wang, Yaqiao Luo, Luxin Zhang, Yinan Zhao, Peter Vajda,  
 790 Dimitris Metaxas, and Licheng Yu. Avid: Any-length video inpainting with diffusion model. *arXiv*  
 791 *preprint arXiv:2312.03816*, 2023b.
- 792 Zicheng Zhang, Bonan Li, Xuecheng Nie, Congying Han, Tiande Guo, and Luoqi Liu. Towards  
 793 consistent video editing with text-to-image diffusion models. In *Advances in Neural Information*  
 794 *Processing Systems (NeurIPS)*, 2023c.
- 795 Lianmin Zheng, Wei-Lin Chiang, Ying Sheng, Siyuan Zhuang, Zhanghao Wu, Yonghao Zhuang,  
 796 Zi Lin, Zhuohan Li, Dacheng Li, Eric Xing, et al. Judging llm-as-a-judge with mt-bench and  
 797 chatbot arena. *Advances in Neural Information Processing Systems*, 36, 2024.
- 798 Luowei Zhou, Chenliang Xu, and Jason Corso. Towards automatic learning of procedures from web  
 799 instructional videos. In *Proceedings of the AAAI Conference on Artificial Intelligence*, 2018a.
- 800 Luowei Zhou, Yingbo Zhou, Jason J Corso, Richard Socher, and Caiming Xiong. End-to-end dense  
 801 video captioning with masked transformer. In *Proceedings of the IEEE conference on computer*  
 802 *vision and pattern recognition*, pp. 8739–8748, 2018b.

810 Yiyang Zhou, Chenhang Cui, Jaehong Yoon, Linjun Zhang, Zhun Deng, Chelsea Finn, Mohit Bansal,  
811 and Huaxiu Yao. Analyzing and mitigating object hallucination in large vision-language models.  
812 In *Proceedings of the International Conference on Learning Representations (ICLR)*, 2024.  
813  
814  
815  
816  
817  
818  
819  
820  
821  
822  
823  
824  
825  
826  
827  
828  
829  
830  
831  
832  
833  
834  
835  
836  
837  
838  
839  
840  
841  
842  
843  
844  
845  
846  
847  
848  
849  
850  
851  
852  
853  
854  
855  
856  
857  
858  
859  
860  
861  
862  
863

## APPENDIX

In this appendix, we present the following:

- More details about VPLM dataset collection (Sec. A.1), experimental setups (Sec. A.2), more implementation details (Sec. A.3).
- Limitations and Negative Societal Impact of RACCoN (Sec. B).
- Additional analysis including ablations (Sec. C.2, Sec. C.1).
- Additional qualitative examples with RACCoN on video content editing (Sec. C.3).

## A EXPERIMENTAL SETUP

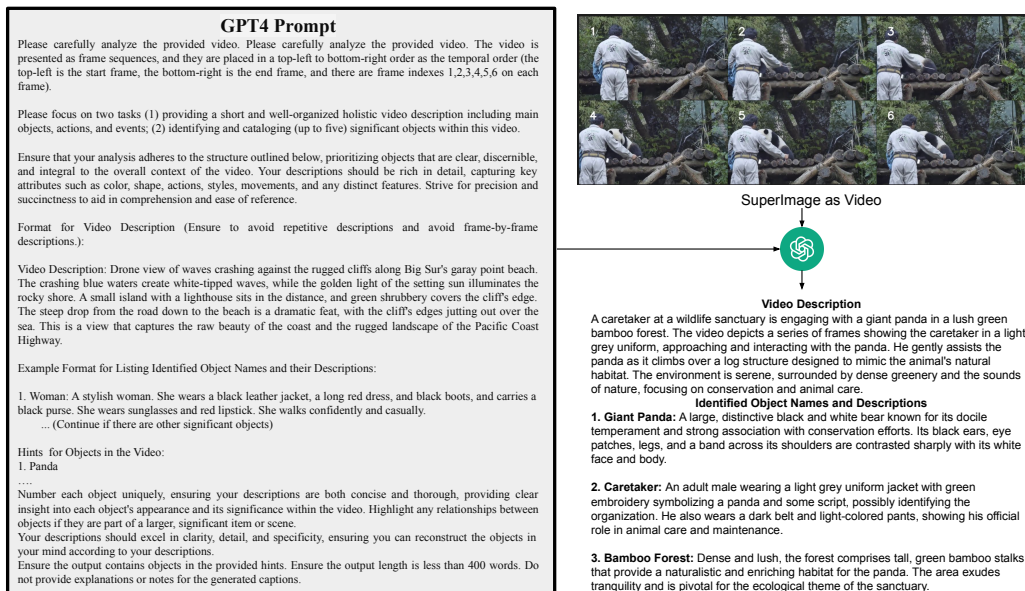


Figure 6: **Pipeline of our VPLM dataset annotation with GPT4V.** We first convert a video as a superimage and then give some in-context examples to prompt GPT-4V to annotate detailed and well-structured video descriptions.

### A.1 VPLM DATA COLLECTION.

As we mention in Sec. 3.3, to facilitate our model training, we start from open-source video inpainting data (Wu et al., 2024)<sup>3</sup> to build a high-quality dataset that includes the well-structured, detailed caption for both video and each object in the video. Specifically, we leverage GPT-4V<sup>4</sup> to annotate each video. As shown in Fig. 6, we first convert a video to a superimage (Fan et al., 2021) by concatenating uniformly sampled frames, and we also draw frame IDs on each frame as a visual prompt to present temporal order. Then we prompt the GPT-4V by providing a detailed prompt with in-context examples (left of Fig. 6). In this case, we obtained well-structured, detailed captions that contain both holistic video and local objects (bottom right of Fig. 6). To ensure the annotation quality, we sampled 1 annotated video from each 100 batches and then did a human cross-check, and refined the batch annotations according to the sampled example. Through this pipeline, we obtained 7.2K high-quality well-structured, detailed video descriptions with an average of 238.0 words for each video.

Next, to obtain paired object-mask-description triplets for video inpainting model training, we build an automatic detailed object caption and object name matching pipeline using GPT4. As in our base

<sup>3</sup>MIT License: <https://choosealicense.com/licenses/mit/>

<sup>4</sup>version 1106

918 dataset (Wu et al., 2024), we already have class labels for each object mask, we framed this matching  
 919 as a multi-choice QA to ask GPT4 which object caption can in Fig. 6 matched to the given object  
 920 classes. We further filtered out the triplets with too small masks (< 1% mask areas.) In this case,  
 921 we obtained 5.5K object-mask-description triplets with an average of 37.2 words for each object to  
 922 support our video diffusion model training.  
 923

## 924 A.2 BENCHMARKS AND DATASETS DETAILS

925 As mentioned in the main paper (??), we evaluate our proposed RACCoN on various tasks.  
 926 For video-to-paragraph generation, we test our model on the standard video caption dataset  
 927 YouCook2 (Zhou et al., 2018a) (validation set) as well as our VPLM dataset. We next test video  
 928 content editing with three subtasks on our VPLM dataset. Regarding the experiments of incorporating  
 929 RACCoN with other conditional video generation models, we test RACCoN on diverse videos  
 930 from ActivityNet, YouCook2, and UCF101. We uniformly selected 100 videos from those 3 datasets  
 931 to build the test bed. For the experiments of incorporating RACCoN with other video editing models,  
 932 we follow the previous work (Geyer et al., 2023), and select 30 unique videos from the DAVIS dataset.  
 933 For each video, we annotate two different types of editing, attribute editing and instance editing. It  
 934 leads to 60 text-video pairs in our video editing evaluation. We choose object captions that contain  
 935 the same keywords for editing in human captions to represent the model-generated caption.  
 936

## 937 A.3 IMPLEMENTATION DETAILS

938 **Metrics:** We provide more details about our metrics. CLIP-Text measures the similarity between  
 939 the edit prompt and the embedding of each frame in the edited video. CLIP-Frame computes  
 940 the average CLIP similarity between the image embeddings of consecutive frames to measure the  
 941 temporal coherency. SSIM measures the structural similarity between the original and edited video  
 942 for evaluating localized editing.  $Q_{edit} = CLIP - T/Wrap - Err$ , it is a comprehensive score for  
 943 video editing quality, where  $Wrap - Err$  calculates the pixel-level difference by warping the edited  
 944 video frames according to the estimated optical flow of the source video, extracted by FlowNet2.0 (Ilg  
 945 et al., 2017). For layout planning, we compute the FVD and CLIP-Image similarity between the  
 946 ground truth and the predicted bounding box.  
 947

948 **More Details about Multi-granular Spatiotemporal Pooling.** As mentioned Sec. 3.1, we proposed  
 949 a novel Multi-granular Spatiotemporal Pooling (MGS Pooling) to address the lack of complex spatial-  
 950 temporal modeling in video. We further provide a more intuitive visualization for our proposed MGS  
 951 Pooling in Fig. 3. We first adopt a lightweight 165 superpixel predictor that generates superpixels  
 952 across video frames, then use the overlapping k-means clustering for the obtained video superpixels.  
 953 In this case, we gather informative cues about various objects and actions for LLM.  
 954

955 **Human Evaluation on Video-to-Paragraph Generation.** We conduct a human evaluation on nine  
 956 randomly selected videos from the YouCook2 dataset. Videos are three- to five-minute-long and  
 957 contain multiple successive scenes with complex viewpoints. We provide these videos to four different  
 958 annotators with ground truth captions, descriptions generated by PG-Video-LLAVA, and our method,  
 959 RACCoN, where the captions/descriptions for each video are randomly shuffled. We leverage  
 960 four distinct human evaluation metrics: Logic Fluency (Logic), Language Fluency (Language),  
 961 Video Summary (Summary) and Video Details (Details). To avoid a misinterpretation of methods'  
 962 capabilities due to relative evaluation, we instruct the annotators to independently rate the quality of  
 963 each set of captions based on these four different criteria, by giving a score from 1 to 5 (i.e., choice:  
 964 [1, 2, 3, 4, 5]).  
 965

966 **Off-shelf Video Editing Models.** We utilize TokenFlow (Geyer et al., 2023) and FateZero (Qi et al.,  
 967 2023) as our video editing tools. TokenFlow generates a high-quality video corresponding to the  
 968 target text, while preserving the spatial layout and motion of the input video. For SSIM computation,  
 969 we compute SSIM for region-of-no-interest since we want to keep those regions unchanged. we  
 970 first mask out regions of interest with the ground truth mask provided by the DAVIS dataset, the we  
 971 compute SSIM on masked images and conduct mean pooling as the video-level metrics.  
 972

973 **Off-shelf Conditional Video Generation Models.** We leverage both VideoCrafter (Chen et al.,  
 974 2023) and DynamiCrafter (Xing et al., 2023) as our video generation backbone. VideoCrafter is  
 975 one of the SoTA video generation models that can handle different input conditions (image, text).  
 976

DynamiCrafter is based on the open-source VideoCrafter and T2I Latent Diffusion model (Rombach et al., 2022), and was trained on WebVid10M (Bain et al., 2021), it provides better dynamic and stronger coherence. We adopt VideoCrafter-512 and DynamiCrafter-512 variants. For each video, we use CLIP similarity to retrieve multiple keyframes corresponding to each caption. Those keyframes result in multiple generated video clips via the video generation model. For FVD computation, we conduct mean pooling over those clips to represent a video. We use  $k = 25$  and  $v = 6$  for generated captions in all experiments. The experiments are conducted on the  $4 \times 48\text{GB}$  A6000 GPUs machine.

## B LIMITATIONS AND BROADER IMPACT

Our proposed RACCoN framework has shown a remarkable ability to interpret input videos, producing well-structured and detailed descriptions that outperform strong video captioning baselines and even ground truths. However, it has the potential to produce inaccuracies or hallucination (Liu et al., 2023a; Wang et al., 2024a; Zhou et al., 2024; Ma et al., 2023) in the generated text outputs. In addition, the performance of our proposed framework in paragraph generation, video generation, and editing is influenced by the employed pre-trained backbones, including an LLM (Touvron et al., 2023), base Inpainting Model (Rombach et al., 2022), Video Diffusion Model (Xing et al., 2023), and Video Editor (Geyer et al., 2023). However, our key contributions are independent of these backbones, and we emphasize that RACCoN’s capabilities can be further enhanced with future advancements in these generative model backbones.

LLM-empowered video description and photorealistic video creation/editing inherit biases from their training data, leading to several broader impacts, including societal stereotypes, biased interpretation of actions, and privacy concerns. To mitigate these broader impacts, it is essential to carefully develop and implement generative and video description models, such as considering diversifying training datasets, implementing fairness and bias evaluation metrics, and engaging communities to understand and address their concerns.

## C ADDITIONAL ANALYSIS

### C.1 ABLATION STUDY

**The effect of  $k$  and  $v$**  As shown in Tab. 7, we did initialized hyperparameter probing experiments on ActivityNet-Cap and YouCook2 datasets. we observe that all variants of our approach with varying  $k$  and  $v$  generally achieve improved performance compared to baselines in terms of multiple video captioning metrics: *SPICE*, *BLEU-4*, *METEOR*, and *ROUGE*. This result demonstrates the efficacy of our multi-granular spatiotemporal pooling approach with a fine to coarse search of video contexts based on superpixels. In addition, we observe that RACCoN framework shows a small gap between variants in each dataset, highlighting the robustness of our approach to the hyperparameter setups and datasets.

**The effect of Superpixel Overlap** We introduce overlapping k-means clustering to aggregate video superpixels, capturing a variety of visual contexts while allowing for partial spatiotemporal overlap. To investigate the effect of our suggested overlapping approach, we also evaluate the variant of our framework without overlap (i.e.,  $v = 1$ ) on video-to-paragraph generation tasks in Tab. 7. As shown, our approach with overlap (i.e.,  $v > 1$ ) surpasses the non-overlapping version of RACCoN across various scales of visual contexts  $k$ , as indicated by the video captioning metrics we evaluated. This emphasizes the advantage of permitting overlap in understanding video contexts, which enhances the input video’s comprehension by allowing for diverse and fluent interpretations of local visual regions with surroundings associated at the same time.

For simplicity, we use  $k = 25$  and  $v = 6$  for all experiments on conditional video generation and video editing tasks, demonstrating the robustness of RACCoN for hyperparameters.

### C.2 COMPARISON WITH PRE-TRAINED GROUNDING MODELS

We further investigate the applicability of recent powerful pre-trained visual grounding models (Kirillov et al., 2023; Cheng et al., 2023; Ren et al., 2024). Segment-Anything (Kirillov et al., 2023)

Table 7: **Ablation of RACCoON** for Video-to-Paragraph Generation on ActivityNet and YouCook2. Metrics are abbreviated: **M**: METEOR, **B**: BLEU-4, **S**: SPICE, **R**: ROUGE.  $v = 1$  indicates the version without superpixel overlap. We highlight the hyperparameter setup used in the main experiment.

Models	$k$	$v$	ActivityNet				YouCook2			
			S	B	M	R	S	B	M	R
PDVC (Wang et al., 2021)	-	-	-	2.6	10.5	-	-	0.8	4.7	-
Vid2Seq (Yang et al., 2023)	-	-	5.4	-	7.1	-	4.0	-	4.6	-
ZeroTA (Jo et al., 2023)	-	-	2.6	-	2.7	-	1.6	-	2.1	-
PG-VL (Munasinghe et al., 2023)	-	-	13.6	13.9	14.2	18.1	6.2	16.5	8.6	15.8
<b>RACCoON</b> (Ours)	25	1	13.5	13.9	14.2	18.1	6.3	16.9	8.7	15.9
		2	13.7	14.6	14.4	18.2	6.4	17.5	8.7	16.1
		4	13.6	14.3	14.3	18.2	6.6	16.2	8.8	16.0
		5	<b>13.8</b>	<b>15.0</b>	<b>14.5</b>	<b>18.4</b>	6.4	17.9	8.8	<b>16.2</b>
		1	13.6	14.1	14.3	18.0	6.1	16.9	8.6	15.9
	30	2	<b>13.8</b>	14.4	14.3	18.3	6.4	16.3	<b>9.0</b>	16.0
		4	13.6	14.3	14.3	18.2	6.6	17.1	8.9	16.1
		6	13.7	14.5	14.4	18.2	<b>6.9</b>	18.0	<b>9.0</b>	16.1
		10	-	-	-	-	6.4	16.5	8.7	16.1
		1	13.6	14.1	14.3	18.0	6.3	16.5	8.8	16.0
	30	2	13.7	14.2	14.2	18.1	6.6	17.1	<b>9.0</b>	<b>16.2</b>
		4	13.5	14.5	14.3	18.2	6.6	<b>18.1</b>	8.8	16.1
		6	13.6	14.4	14.4	18.2	6.4	17.2	8.8	<b>16.2</b>

Table 8: **RACCoON variants with different grounding methods** for Video-to-Paragraph Generation on YouCook2.

Method	Localization	Clustering	SPICE	BLEU-4	METEOR	ROUGE
PG-VL (Munasinghe et al., 2023)	-	-	6.2	16.5	8.6	15.8
Ours	SAM (Kirillov et al., 2023)	-	6.4	16.9	8.7	15.9
	Grounded SAM (Ren et al., 2024)	-	6.5	16.5	8.7	<b>16.1</b>
	SAM-Track (Cheng et al., 2023)	k-means	6.2	16.5	8.8	<b>16.1</b>
	SAM-Track (Cheng et al., 2023)	overlapping k-means	6.5	17.4	<b>9.0</b>	<b>16.1</b>
	Superpixel	overlapping k-means	<b>6.9</b>	<b>18.0</b>	<b>9.0</b>	<b>16.1</b>

and Grounded SAM (Ren et al., 2024) are strong open-ended object segmentation models for images, and we directly compute our localized granular tokens based on their segmentation masks. We select 25 segmentation masks in total, from uniformly sampled frames in each video for fair comparison with RACCoON ( $k = 25$ ). As shown in Tab. 8, these variants of RACCoON achieve improved performance against the best-performing baseline, PG-VL, but are often suboptimal since they focus on regional information and cannot contain temporal information of the videos. Unlike these image-based segmentation methods, SAM-Track (Cheng et al., 2023) generates coherent masks of observed objects over successive frames in videos, by adopting multiple additional pre-trained modules, including GroundingDino (Liu et al., 2023d) and AOT (Yang et al., 2021; Yang & Yang, 2022). We adopt SAM-Track to initialize superpixels in videos and conduct overlapping k-means clustering ( $k = 25$ ). Here, we observe that RACCoON with SAM-Track superpixel initialization achieves reasonable performance, and is beneficial for video editing tasks. It enables the model to coherently edit targeted regions in videos with edited keywords.

### C.3 ADDITIONAL VISUALIZATIONS

In this section, we provide more qualitative examples of various tasks, including three types of video content editing, ablation on removing oracle planning and GT masks, enhanced video editing, and conditional video generation.

**Remove, Add, and Change Object the videos.** We provide more qualitative examples in this Appendix across different types of video content editing (Fig. 7), including removing (Fig. 8, Fig. 9, Fig. 10), adding (Fig. 11, Fig. 12, Fig. 13), and changing/editing (Fig. 14, Fig. 15, Fig. 16). According to the visualization, our RACCoON generally outperforms other strong baselines on all three subtasks. Our RACCoON can reflect the updated text description more accurately, thus aiding in a user-friendly video-generative framework. For example, our method can accurately change the color of the hat (*red*→*blue*), which is a very small area in the video, while other methods struggle to meet the requirement.

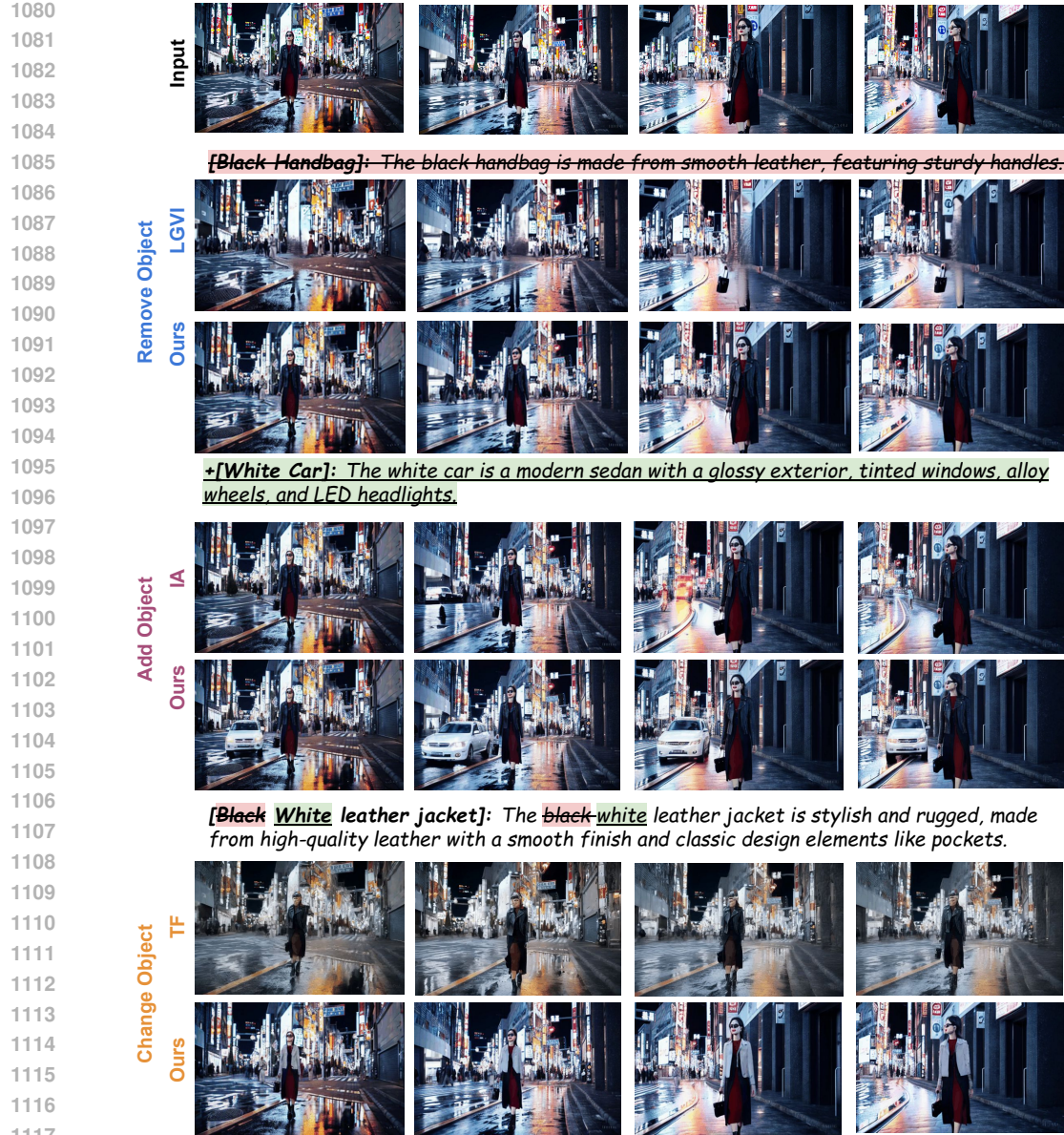


Figure 7: More visualization of diverse editing skills on Sora video and comparison with other methods

**Ablation Study Visualization.** We illustrate extra visualizations for replacing oracle mask with grounding&tracking tools generated ones for video object removal (Fig. 17 and Fig. 18) and changing (Fig. 19 and Fig. 20), as well as replacing oracle object boxes with our model-predicted one (Fig. 21 and Fig. 22). Our framework shows robust results with LLM planning and off-shelf segmentation tools. We further show the failure cases of removing and changing objects mainly come from the missing mask prediction of the video segmentation masks.

1134

1135

1136

1137

1138

1139

1140

1141

1142

1143

1144

1145

1146

1147

1148

1149

1150

1151

1152

1153

1154

1155

1156

1157

1158

1159

1160

1161

1162

1163

1164

1165

1166

1167

1168

1169

1170

1171

1172

1173

1174

1175

1176

1177

1178

1179

1180

1181

1182

1183

1184

1185

1186

1187

Input



*[Observer]: A male wearing dark grey shorts, a black T shirt with neon yellow logos and athletic shoes. He stands attentively with his arms crossed, watching the shooter's performance background*

VC



LGV



Ours



Input



*[White Poodle]: A small, fluffy white poodle exhibiting a pampered and stylized appearance with a rounded haircut characteristic of the breed's show grooming standards. The dog moves with a deliberate prance, displaying the distinctive behavior and training fit for a show animal background*

VC



LGV



Ours

Figure 8: More visualization of **removing** video objects

1188

1189

1190

1191

1192

1193

1194

1195

1196

1197

1198

**Input**

**[Seagull]:** A white seagull with wings spread wide, showcasing gray tips. As it flies, its yellow beak and black eye markings are noticeable, adding to its distinctive features. The bird's underbelly is white, reflecting sunlight, while the light and smooth lines of its body exemplify a strong yet graceful figure in mid flight. background

**VC****LGV1****Ours****Input**

**[Large Shark]:** A sizable and powerful shark, possibly a Great White, with a grey and white body. Its dorsal fin is tall and prominent, and it has a distinctly streamlined shape. The shark conveys a sense of calm authority as it moves effortlessly through the water. background

**VC****LGV1****Ours**Figure 9: More visualization of **removing** video objects

1239

1240

1241

1242

1243

1244

1245

1246

1247

1248

1249

1250

1251

1252

1253

1254

1255

1256

1257

1258

1259

1260

1261

1262

1263

1264

1265

1266

1267

1268

1269

1270

1271

1272

1273

1274

1275

1276

1277

1278

1279

1280

1281

1282

1283

1284

1285

1286

1287

1288

1289

1290

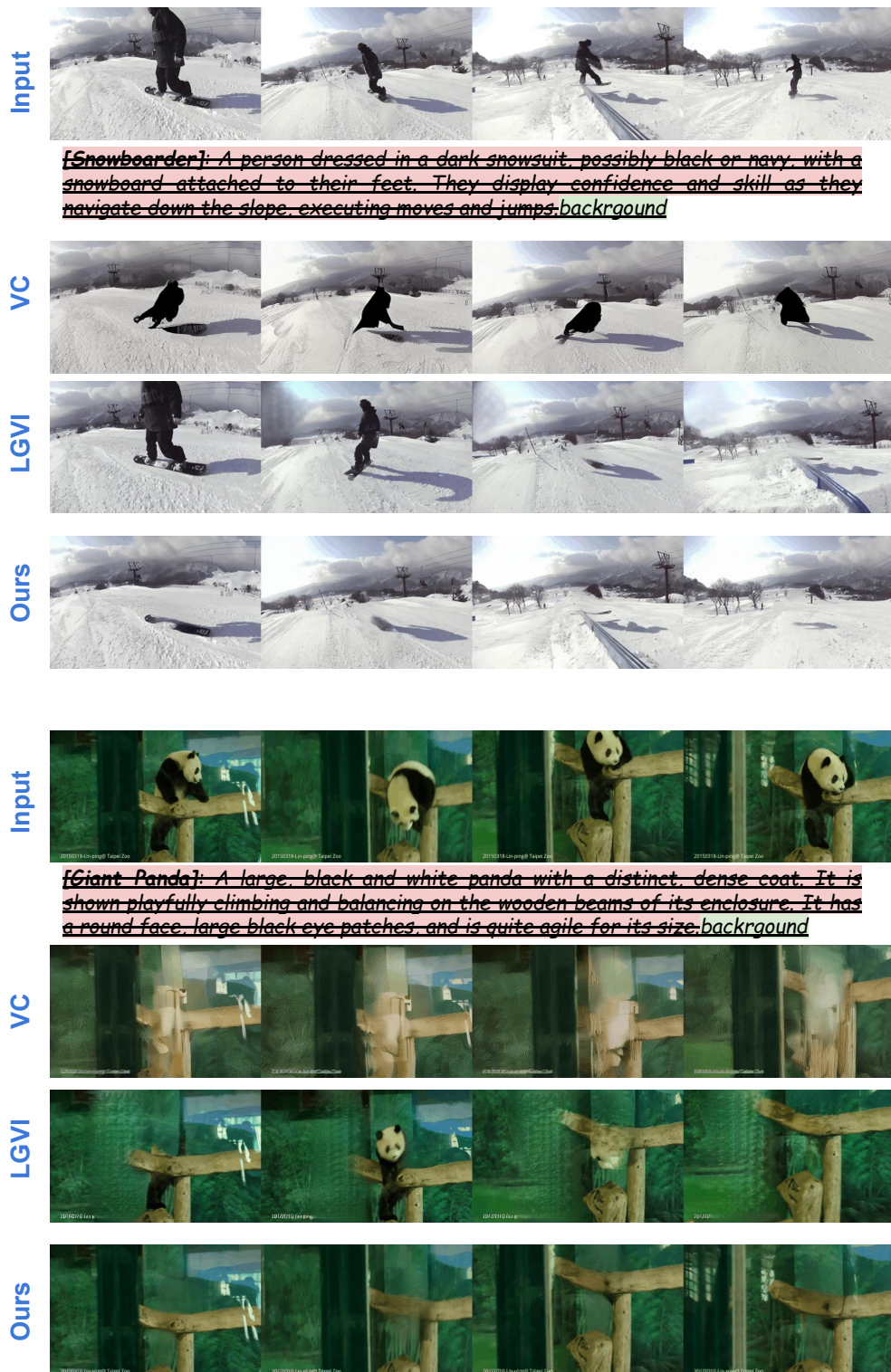
1291

1292

1293

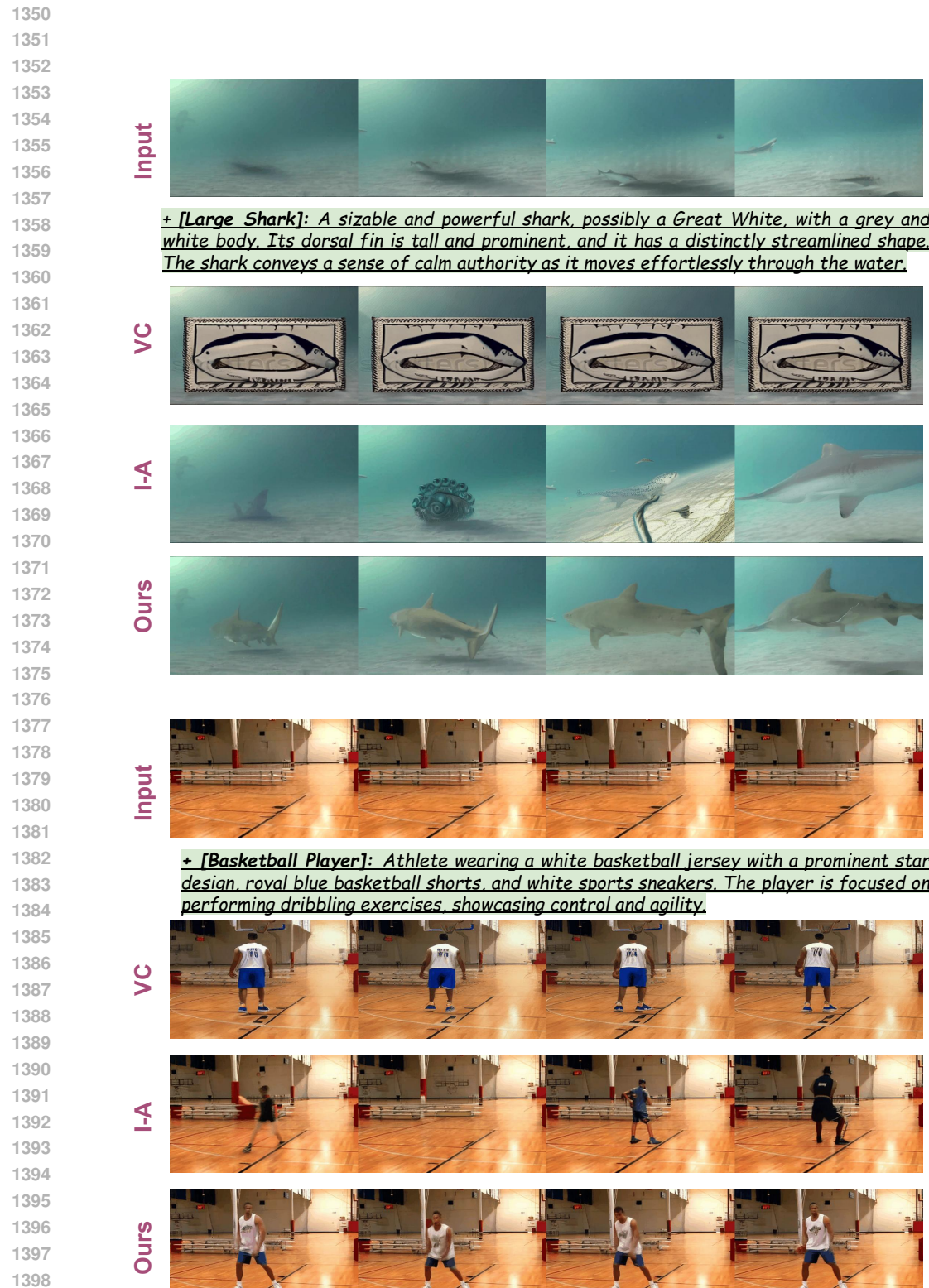
1294

1295

Figure 10: More visualization of **removing** video objects

1296  
 1297  
 1298  
 1299  
 1300  
 1301  
 1302  
 1303  
 1304  
 1305  
 1306  
 1307  
 1308  
 1309  
 1310  
 1311  
 1312  
 1313  
 1314  
 1315  
 1316  
 1317  
 1318  
 1319  
 1320  
 1321  
 1322  
 1323  
 1324  
 1325  
 1326  
 1327  
 1328  
 1329  
 1330  
 1331  
 1332  
 1333  
 1334  
 1335  
 1336  
 1337  
 1338  
 1339  
 1340  
 1341  
 1342  
 1343  
 1344  
 1345  
 1346  
 1347  
 1348  
 1349

Figure 11: More visualization of **adding** video objects

Figure 12: More visualization of **adding** video objects

1404

1405

1406

1407

1408

1409

1410

1411

1412

1413

1414

**Input**

+ **[Seagull]**: A white seagull with wings spread wide, showcasing gray tips. As it flies, its yellow beak and black eye markings are noticeable, adding to its distinctive features. The bird's underbelly is white, reflecting sunlight, while the light and smooth lines of its body exemplify a strong yet graceful figure in mid-flight.

**VC****I-A****Ours****Input**

+ **[Brown Dog]**: An enthusiastic medium-sized brown dog with glossy fur and a lean build. It remains undeterred by the splashes, focused on the man and possibly a tossed object or on the interaction itself. Its tail is partially submerged, blending into the blue water, and it moves swiftly, demonstrating agility and the enjoyment of water.

**VC****I-A****Ours**Figure 13: More visualization of **adding** video objects

1455

1456

1457

1458

1459

1460

1461

1462

1463

1464

1465

1466

1467

1468

1469

1470

1471

1472

1473

1474

1475

1476

1477

1478

1479

1480

1481

1482

1483

1484

1485

1486

1487

1488

1489

1490

1491

1492

1493

1494

1495

1496

1497

1498

1499

1500

1501

1502

1503

1504

1505

1506

1507

1508

1509

1510

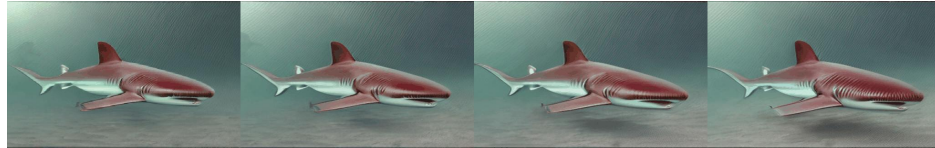
1511

Input

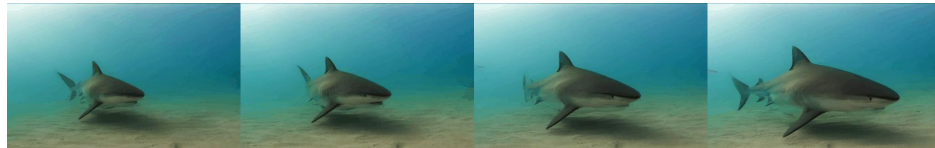


**[Large-Shark] [Orange Shark]:** A sizable and powerful shark, possibly a Great White, with a grey and white-orange body. Its dorsal fin is tall and prominent, and it has a distinctly streamlined shape. The shark conveys a sense of calm authority as it moves effortlessly through the water.

VC



TF



Ours



Input



**[Man] [Man in orange]:** An athletic man wearing an orange shirt, black white shorts, and sports shoes. He is running on a well-maintained playing area characterized by manicured green grass, a smooth outfield, and a perimeter wall adorned with sponsorship banners and a scoreboard.

VC



TF



Ours



Figure 14: More visualization of **editing** video objects

1512

1513

1514

1515

1516

1517

1518

1519

1520

1521

1522

1523

1524

1525

1526

1527

1528

1529

1530

1531

1532

1533

1534

1535

1536

1537

1538

1539

1540

1541

1542

1543

1544

1545

1546

1547

1548

1549

1550

1551

1552

1553

1554

1555

1556

1557

1558

1559

1560

1561

1562

1563

1564

1565

Input



**[Player 1 with Red Hat]** [Player 1 with Blue Hat]: Male player on the near side of the court. He is wearing a white shirt, dark shorts, and a red blue hat, and is playing with a yellow tennis racket. He serves and returns the ball, demonstrating agility and competitive spirit in the game.

VC



TF



Ours



Input



**[Person]:** Clad in a dark-colored jacket colorful, rainbow-striped jacket and pants, the person assumes a casual yet attentive posture while walking the dog, indicative of a routine stroll.

VC



TF



Ours



Figure 15: More visualization of **editing** video objects

1566

1567

1568

1569

1570

1571

1572

1573

1574

1575

1576

1577

1578

1579

1580

1581

1582

1583

1584

1585

1586

1587

1588

1589

1590

1591

1592

1593

1594

1595

1596

1597

1598

1599

1600

1601

1602

1603

1604

1605

1606

1607

1608

1609

1610

1611

1612

1613

1614

1615

1616

1617

1618

1619

**Input**

**[Baby Gorilla] [Baby Panda]**: A young **gorilla** panda with black fur, portrayed in the act of crawling. The gorilla's movement is slow and cautious, exhibiting natural curiosity as it explores its surroundings.

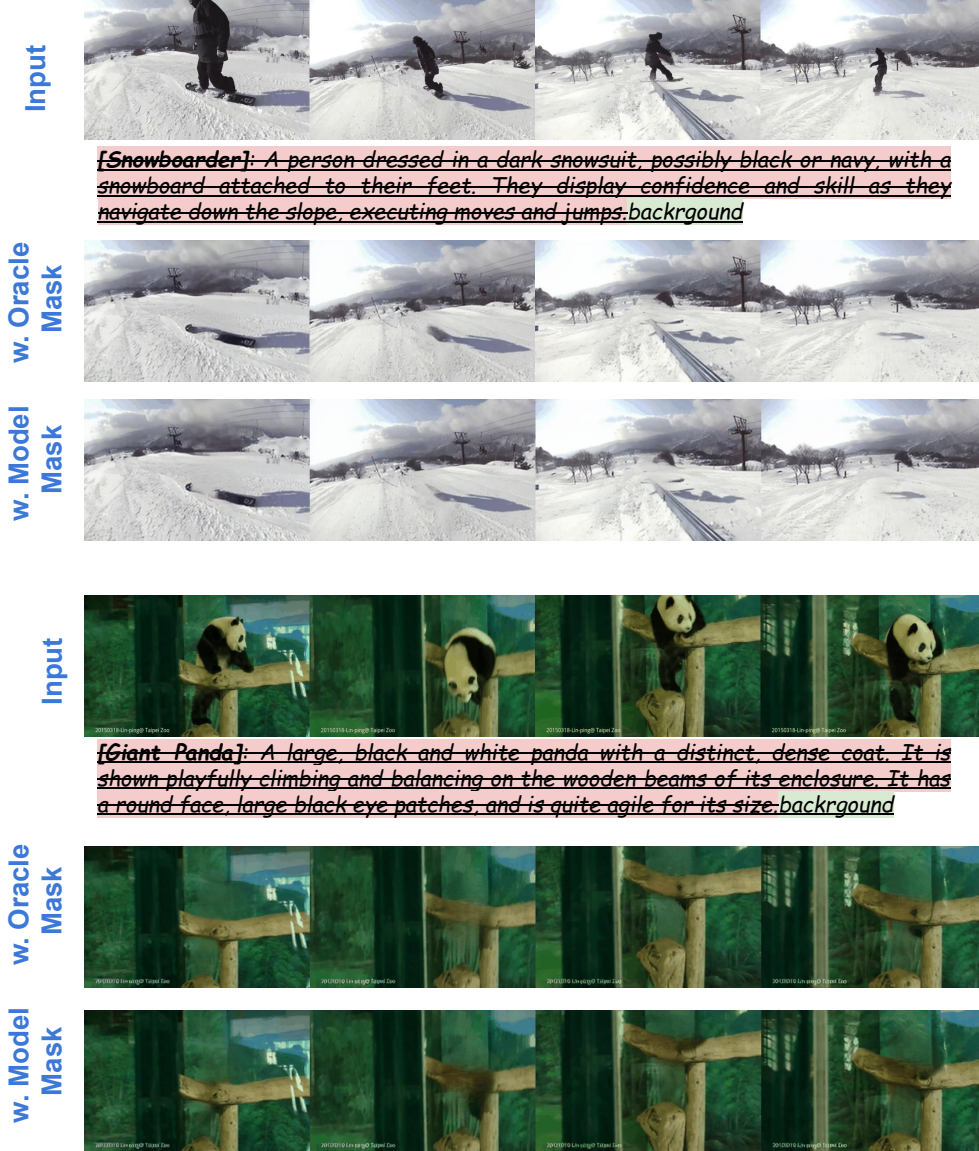
**VC****TF****Ours****Input**

**[Dalmatian] [Dog]**: A medium-sized, **Dalmatian** dog with white facial markings, a white chest, and white-tipped paws. It has floppy ears, a long tail, and a gentle expression. The dog is actively engaging with a ball, using its front paws and nose, displaying playful behavior.

**VC****TF****Ours**

Figure 16: More visualization of **editing** video objects

1620  
 1621  
 1622  
 1623  
 1624  
 1625  
 1626  
 1627  
 1628  
 1629  
 1630  
 1631  
 1632  
 1633  
 1634  
 1635  
 1636  
 1637  
 1638  
 1639  
 1640  
 1641  
 1642  
 1643  
 1644  
 1645  
 1646  
 1647  
 1648  
 1649  
 1650  
 1651  
 1652  
 1653  
 1654  
 1655  
 1656  
 1657  
 1658  
 1659  
 1660  
 1661  
 1662  
 1663  
 1664  
 1665  
 1666  
 1667  
 1668  
 1669  
 1670  
 1671  
 1672  
 1673

Figure 17: More visualization of **removing** video objects

1674

1675

1676

1677

1678

1679

1680

1681

1682

1683

1684

1685

1686

**[Snowboarder]:** A person dressed in a dark snowsuit, possibly black or navy, with a snowboard attached to their feet. They display confidence and skill as they navigate down the slope, executing moves and jumps. background



1687

1688

1689

1690

1691

1692

1693

1694

1695

1696

1697

1698

1699

1700

1701

1702

1703

1704

1705

1706

1707

1708

1709

1710

1711

1712

1713

1714

1715

1716

1717

1718

1719

1720

1721

1722

1723

1724

1725

1726

1727

Input

w. Oracle  
Maskw. Model  
Mask

Input



**[Giant Panda]:** A large, black and white panda with a distinct, dense coat. It is shown playfully climbing and balancing on the wooden beams of its enclosure. It has a round face, large black eye patches, and is quite agile for its size. background

w. Oracle  
Maskw. Model  
MaskFigure 18: More visualization of **removing** video objects

1728  
 1729  
 1730  
 1731  
 1732  
 1733  
 1734  
 1735  
 1736  
 1737  
 1738  
 1739  
 1740  
 1741  
 1742  
 1743  
 1744  
 1745  
 1746  
 1747  
 1748  
 1749  
 1750  
 1751  
 1752  
 1753  
 1754  
 1755  
 1756  
 1757  
 1758  
 1759  
 1760  
 1761  
 1762  
 1763  
 1764  
 1765  
 1766  
 1767  
 1768  
 1769  
 1770  
 1771  
 1772  
 1773  
 1774  
 1775  
 1776  
 1777  
 1778  
 1779  
 1780  
 1781

**Input**  
**w. Oracle Mask**  
**w. Model Mask**  
**Input**  
**w. Oracle Mask**  
**w. Model Mask**



Figure 19: More visualization of **editing** video objects

1782  
 1783  
 1784  
 1785  
 1786  
 1787  
 1788  
 1789  
 1790  
 1791  
 1792  
 1793  
 1794  
 1795  
 1796  
 1797  
 1798  
 1799  
 1800  
 1801  
 1802  
 1803  
 1804  
 1805  
 1806  
 1807  
 1808  
 1809  
 1810  
 1811  
 1812  
 1813  
 1814  
 1815  
 1816  
 1817  
 1818  
 1819  
 1820  
 1821  
 1822  
 1823  
 1824  
 1825  
 1826  
 1827  
 1828  
 1829  
 1830  
 1831  
 1832  
 1833  
 1834  
 1835

**Input**  
**w. Oracle Mask**  
**w. Model Mask**



**[Large Shark] [Orange Shark]:** A sizable and powerful shark, possibly a Great White, with a grey and white-orange body. Its dorsal fin is tall and prominent, and it has a distinctly streamlined shape. The shark conveys a sense of calm authority as it moves effortlessly through the water.



**Input**  
**w. Oracle Mask**  
**w. Model Mask**



**[Woman]:** Dressed in a casual outfit of blue denim shorts and a horizontally striped blue and white T-shirt **a dark red dining dress**. She accessorizes with pink flip-flops and is engaged in the action of putting a leash on her dog, showing signs of preparing for a walk.



Figure 20: More visualization of **editing** video objects

1836  
 1837  
 1838  
 1839  
 1840  
 1841  
 1842  
 1843  
 1844  
 1845  
 1846  
 1847  
 1848  
 1849  
 1850  
 1851  
 1852  
 1853  
 1854  
 1855  
 1856  
 1857  
 1858  
 1859  
 1860  
 1861  
 1862  
 1863  
 1864  
 1865  
 1866  
 1867  
 1868  
 1869  
 1870  
 1871  
 1872  
 1873  
 1874  
 1875  
 1876  
 1877  
 1878  
 1879  
 1880  
 1881  
 1882  
 1883  
 1884  
 1885  
 1886  
 1887  
 1888  
 1889

**Input**  
**w. Oracle Planning**  
**w. Model Planning**  
**Input**  
**w. Oracle Planning**  
**w. Model Planning**

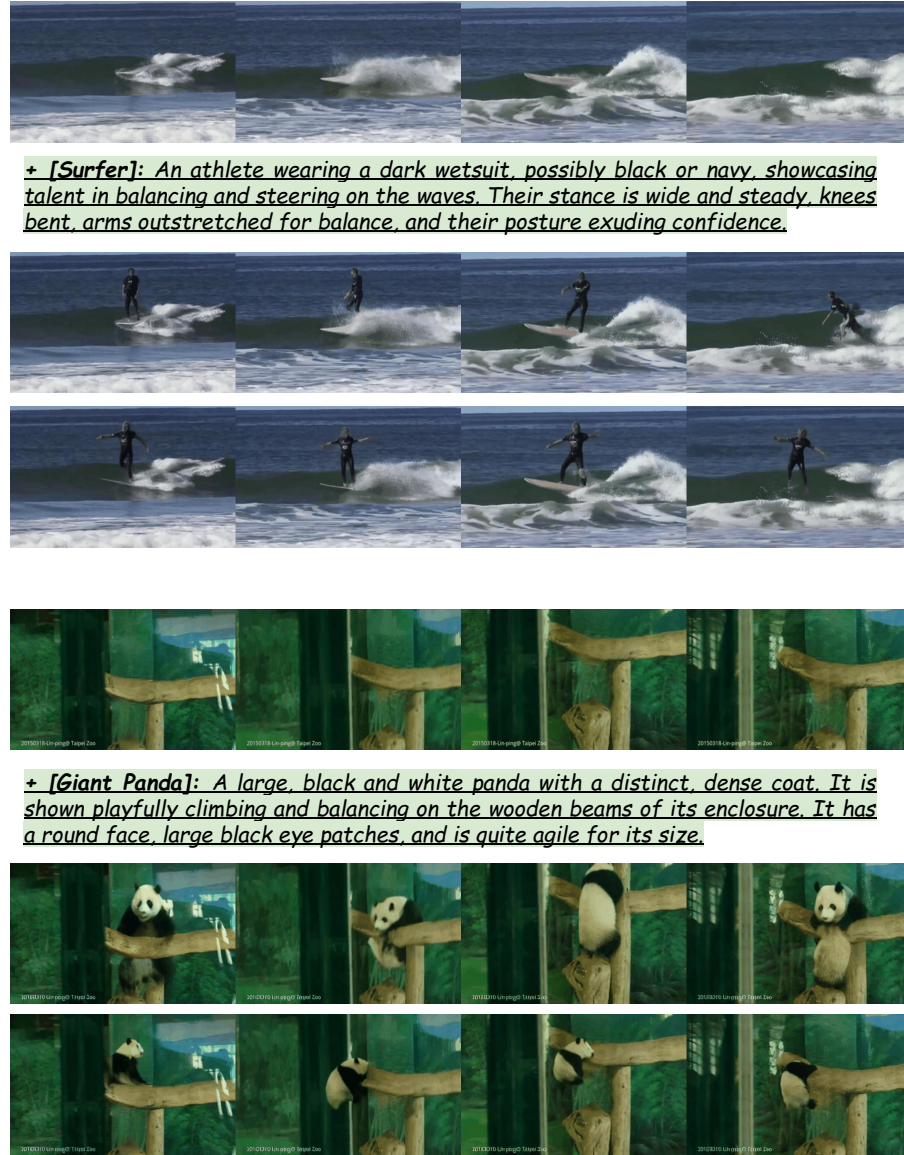


Figure 21: More visualization of **adding** video objects

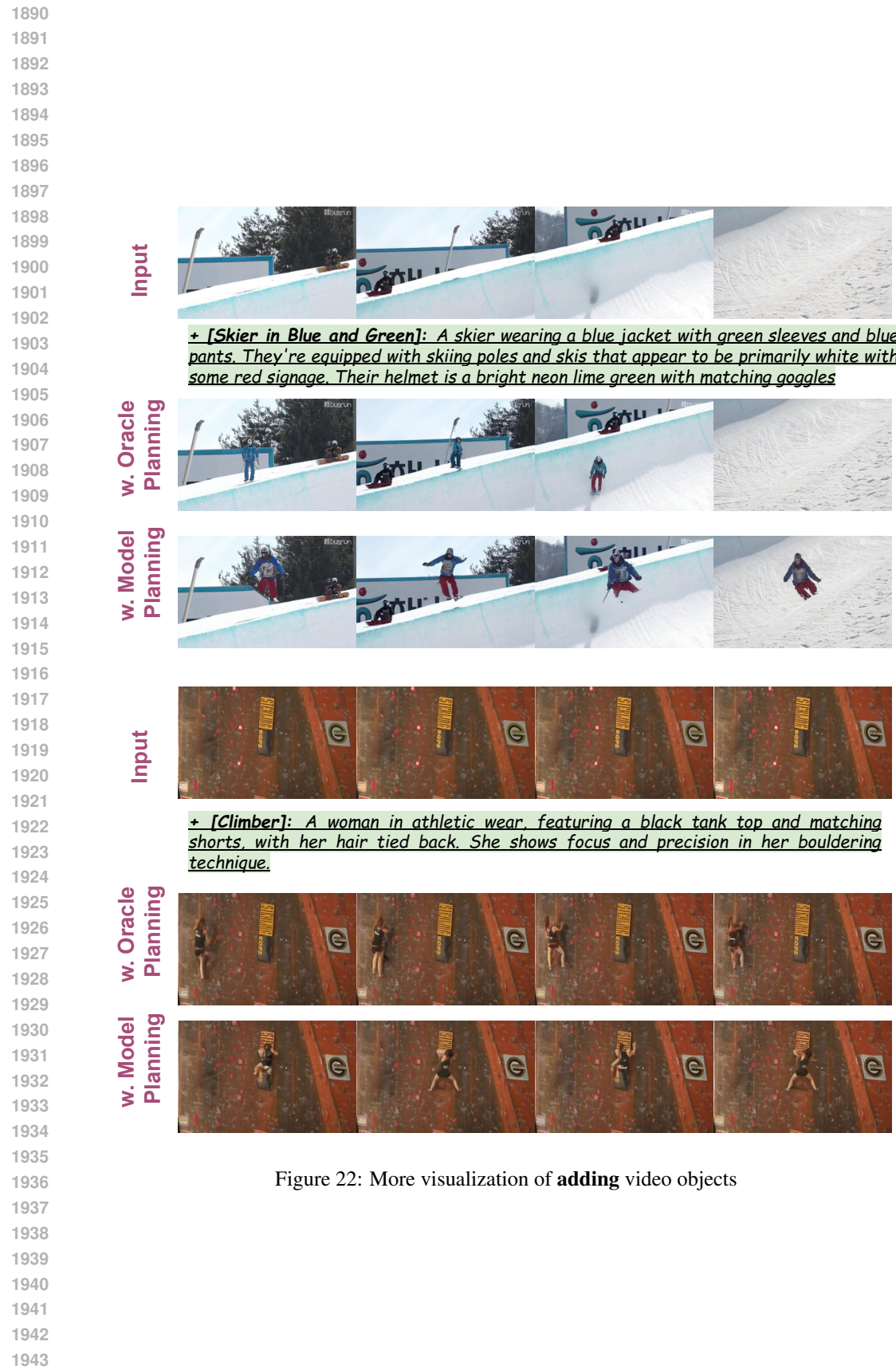
Figure 22: More visualization of **adding** video objects



Figure 23: **Visualization of text-based video editing.** The edited words are marked with **Red**, and the target words are marked with **Green**. The RACCoON caption is selected from predicted dense captions. We highlight the region of interest with red dashed-line boxes for comparison.

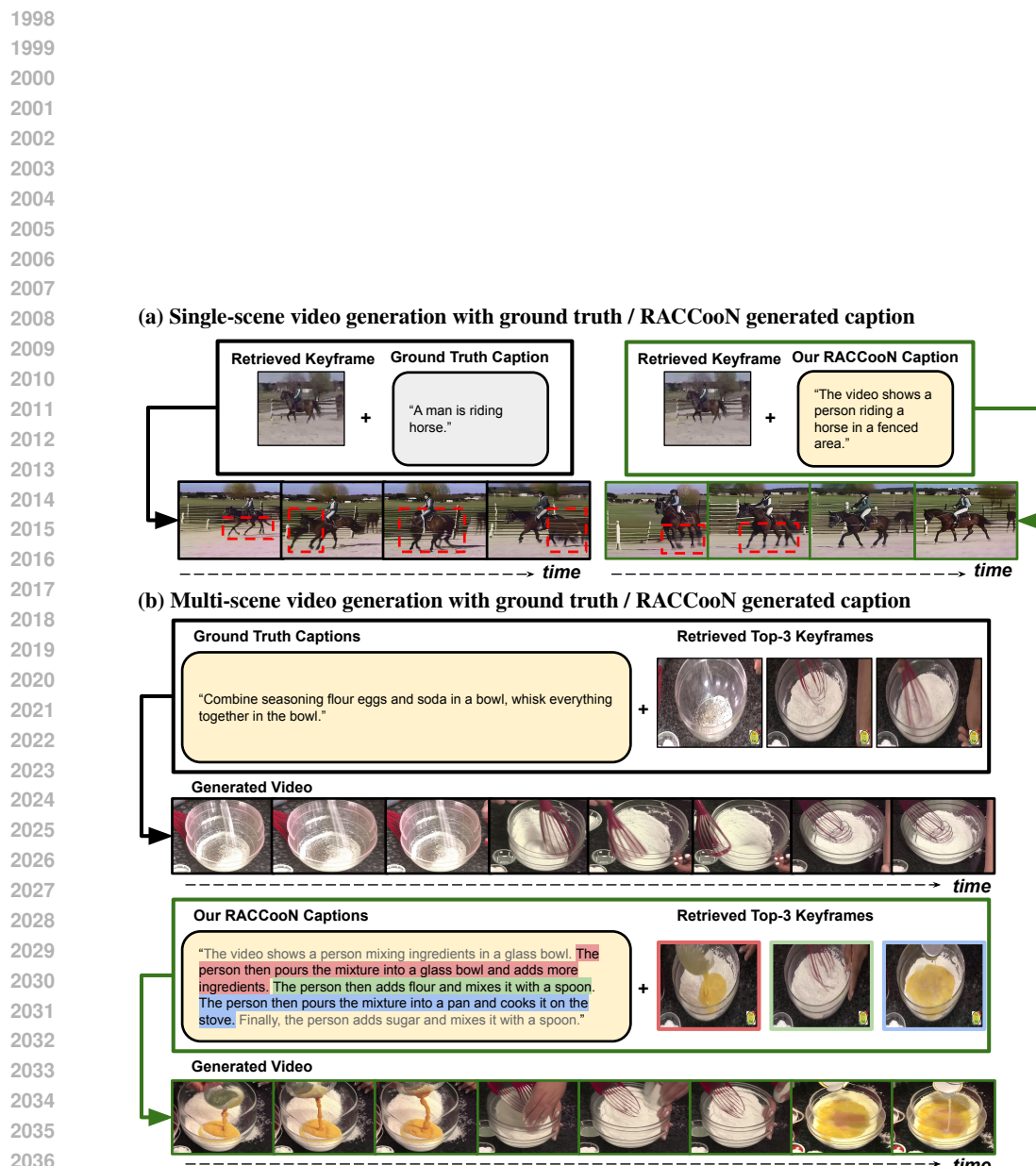


Figure 24: **Visualization of conditional video generation with VideoCrafter.** Top (a): we compare generation results conditional on different captions and with the **same** keyframe. Bottom (b): we leverage multiple keyframes retrieved by different captions to generate multi-scene video. We gray out captions that are not used for retrieval, and highlight captions used for keyframe retrieval. We highlight the region of distortion with red dashed-line boxes for detailed comparison.

2052  
2053  
2054  
2055  
2056  
2057  
2058  
2059  
2060  
2061  
2062  
2063  
2064  
2065  
2066  
2067  
2068  
2069



Masks of Handbag



Masks of Jacket



Figure 25: **Visualization of Masks.**